

AD-A020 991

ANALYSIS OF ARBITRARILY ORIENTED THIN WIRE ANTENNA
ARRAYS OVER IMPERFECT GROUND PLANES

Tapan K. Sarkar, et al

Syracuse University

Prepared for:

Air Force Cambridge Research Laboratories

December 1975

DISTRIBUTED BY:

NTIS

National Technical Information Service
U. S. DEPARTMENT OF COMMERCE

061141

AFCEL-TR-75-0641

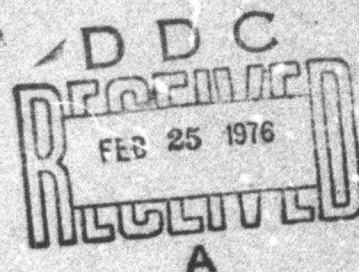
**ANALYSIS OF ARBITRARILY ORIENTED THIN WIRE ANTENNA
ARRAYS OVER IMPERFECT GROUND PLANES**

by

**Tapan K. Sarkar
Bradley J. Strait**

**Department of
Electrical and Computer Engineering
Syracuse University
Syracuse, New York 13210**

**Scientific Report No. 9
December 1975**



Approved for public release; distribution unlimited

**AIR FORCE CAMBRIDGE RESEARCH LABORATORIES
AIR FORCE SYSTEMS COMMAND
UNITED STATES AIR FORCE
HANSCOM AFB, MASSACHUSETTS 01731**

Reproduced by

**NATIONAL TECHNICAL
INFORMATION SERVICE**

U S Department of Commerce
Springfield VA 22151

UNCLASSIFIED

Security Classification		DOCUMENT CONTROL DATA - R & D	
(Security classification of title, body of abstract and indexing annotation must be entered when the overall report is classified)			
1. ORIGINATING ACTIVITY (Corporate author) Syracuse University Department of Electrical & Computer Engineering Syracuse, New York 13210		2a. REPORT SECURITY CLASSIFICATION UNCLASSIFIED	
		2b. GROUP	
3. REPORT TITLE ANALYSIS OF ARBITRARILY ORIENTED THIN WIRE ANTENNA ARRAYS OVER IMPERFECT GROUND PLANES			
4. DESCRIPTIVE NOTES (Type of report and inclusive dates) Scientific, Interim			
5. AUTHOR(S) (First name, middle initial, last name) Tapan K. Sarkar Bradley J. Strait			
6. REPORT DATE December 1975	7a. TOTAL NO. OF PAGES 106	7b. NO. OF REFS 36	
8a. CONTRACT OR GRANT NO. F19628-73-C-0047	8b. ORIGINATOR'S REPORT NUMBER(S) Scientific Report No. 9		
8c. PROJECT, TASK, AND WORK UNIT NO. 5635-06-01	8d. OTHER REPORT NO(S) (Any other numbers that may be assigned this report) AFCRL-TR-75-0641		
8e. DOD ELEMENT 61102F			
8f. DOD SUBELEMENT 681305			
10. DISTRIBUTION STATEMENT A - Approved for public release; distribution unlimited.			
11. SUPPLEMENTARY NOTES TECH, OTHER		12. SPONSORING MILITARY ACTIVITY Air Force Cambridge Research Laboratories Hanscom AFB, Massachusetts 01731 Contract Monitor: Peter R. Franchi/LZR	
13. ABSTRACT This work considers the analysis of antenna and arrays of thin wires of arbitrary orientation above imperfectly conducting ground planes. Emphasis is placed on the development of fast and accurate techniques for computation of the characteristics of antenna systems. An important problem is the evaluation of certain semi-infinite integrals encountered in the exact Sommerfeld solution. The time required for computation of these integrals is reduced by the application of interpolatory quadrature formulas. Where applicable, a modified method of steepest descent is used to evaluate the integrals. The approximate reflection coefficient method is derived from the Sommerfeld formulation via the method of steepest descent. The accuracy of the reflection coefficient method relative to the Sommerfeld method is discussed. Finally, formulas convenient for the optimization of various performance indices are discussed. Typical indices that have been optimized, both with and without constraints, are directivity, power gain, quality factor, and main beam radiation efficiency.			

DD FORM 1 NOV 66 1473

UNCLASSIFIED

Security Classification

14 KEY WORDS	LINK A		LINK B		LINK C	
	ROLE	WT	ROLE	WT	ROLE	WT
Antennas over ground						
Arrays over ground						
Dipoles over ground						
Imperfect ground planes						
Method of steepest descent						
Optimization of arrays over ground						
Reflection coefficient method						
Sommerfeld's method						
Wire antennas over ground						

ACKNOWLEDGEMENT

The author is very much indebted to his research supervisor Dr. B. J. Strait for his keen interest and assistance throughout the course of the project.

Grateful acknowledgement is made to Dr. R. F. Harrington, Dr. H. Gruenberg, and Dr. J. Mautz for their constant assistance and helpful suggestions.

The author is grateful to the National Science Foundation and Air Force Cambridge Research Laboratories for a Research Assistantship during the period 1972-1975.

Finally, the author also wishes to thank Mrs. Gladys Stith for expertly typing the manuscript.

CONTENTS

	Page
1. INTRODUCTION-----	1
2. VERTICAL DIPOLES OVER THE HORIZONTAL PLANE SURFACE OF IMPERFECT GROUND-----	4
2.1. Sommerfeld Formulation-----	4
2.2. Analysis of the Reflected Field-----	10
a) Exact Solution-----	11
b) Reflection-Coefficient Method-----	13
c) Fields Near the Interface-----	24
2.3. Evaluation of Mutual Impedance between two Parallel Vertical Dipoles Situated Over a Plane Imperfect Ground-----	28
2.4. Conclusion-----	32
3. HORIZONTAL DIPOLES OVER A PLANE IMPERFECT GROUND-----	34
3.1. Sommerfeld Formulation-----	34
3.2. Evaluation of Mutual Impedance between Two Parallel Horizontal Dipoles-----	40
3.3. Numerical Evaluation of the Integrals-----	43
a) Exact Solution-----	43
b) Modified Method of Steepest Descent-----	44
3.4. Reflection-Coefficient Method-----	45
3.5. Comparison of Accuracy between the Reflection Coefficient Method and the Exact Sommerfeld Formulation-----	48
3.6. Conclusion-----	51
4. ARBITRARY ORIENTED WIRE ANTENNAS OVER IMPERFECT GROUND---	53
4.1. Exact Sommerfeld Formulation-----	53
4.2. Reflection-Coefficient Method-----	57
4.3. Validity of the Reflection Coefficient Method as Compared with the Exact Solution-----	60
4.4. Conclusion-----	61

	Page
5. OPTIMIZATION METHODS FOR ARBITRARILY ORIENTED ARRAYS OF ANTENNAS OVER IMPERFECT GROUND-----	62
5.1. Gain Maximization-----	64
5.2. Efficiency Indices-----	67
5.3. Quality Factor-----	69
5.4. Optimization Subject to Constraint on Pattern Nulls in the Upper Half Space-----	70
5.5. Optimization Subject to Constraints on the Resulting Sidelobes in the Upper Half Space-----	73
5.6. Optimization of One Performance Index Subject to a Constraint on Another-----	76
5.7. Optimization with Respect to Antenna Geometry-----	80
5.8. Optimizations of Loaded Antennas-----	81
6. CONCLUSION-----	83
APPENDICES	
A. QUADRATURES OF THE HIGHEST ALGEBRAIC ACCURACY-----	85
B. ASYMPTOTIC EVALUATION OF INTEGRALS BY THE METHOD OF STEEPEST DESCENT-----	93
REFERENCES-----	97

1. INTRODUCTION

The objective of this work is to develop fast, accurate techniques to determine the characteristics of wire antennas over plane imperfect ground. Since Sommerfeld, who first analyzed the problem in 1908, numerous papers and articles have been written by several different authors. A good bibliography for this general area can be found in the book by Banõs [1]. Recently, Miller et al [2,3], Lytle and Lager [4,5] developed user oriented computer programs for analysis of the electromagnetic characteristics of arbitrary wire configurations over imperfect ground. With the aid of these general purpose programs one can easily solve for input impedances, current distributions, and field patterns of wire antennas operating in the presence of a plane imperfectly conducting earth. This thesis deals with some useful revisions and improvements of their work.

-
- [1] A. Banõs, "Dipole Radiation in the Presence of a Conducting Half-Space," Pergamon Press, New York 1966.
 - [2] E. K. Miller, A. J. Pozzio, G. J. Burke and E. S. Selden, "Analysis of Wire Antennas in the Presence of a Conducting Half-Space: Part I. The Vertical Antenna in Free Space," Canadian J. of Physics, vol. 50, pp. 879-888, 1972.
 - [3] E. K. Miller, A. J. Pozzio, G. J. Burke and E. S. Selden, "Analysis of Wire Antennas in the Presence of Conducting Half-Space: Part II. The Horizontal Antenna in Free Space," Canadian J. of Physics, vol. 50, pp. 2614-2627, 1972.
 - [4] D. L. Lager and R. J. Lytle, "Numerical Evaluation of Sommerfeld Integrals," Lawrence Livermore Laboratory, "Rept. UCRL-51688, October 23, 1974.
 - [5] D. L. Lager and R. J. Lytle, "Fortran Subroutines for the Numerical Evaluation of Sommerfeld Integrals Unter Aderemem," Lawrence Livermore Laboratory, "Rept. UCRL-51821, May 21, 1975.

The major problem in developing a general purpose program to approach the problem at hand is the required evaluation of certain semi-infinite integrals encountered in the exact Sommerfeld formulation. In this work an efficient method is applied to integrate the semi-infinite integrals in an essentially exact way. The method applied involves the use of orthogonal interpolatory polynomials of highest algebraic accuracy. Where applicable, a modified method of steepest descent has been applied to evaluate these semi-infinite integrals to reduce the time of computation without significant loss of accuracy. In addition a method of steepest descent has been used to obtain the reflection coefficient method as the leading term in the series resulting from the integration of the semi-infinite integrals. Since the reflection coefficient method is very easy to apply it is useful to examine its relative accuracy.

Finally methods are presented here for optimizing certain performance indices of arrays of arbitrarily oriented wire antennas operating over imperfectly conducting ground. The indices considered include directivity, maximum power gain, quality factor, and the efficiency index referred to as main beam radiation efficiency. Optimization problems both with and without constraints on the resulting antenna pattern are illustrated. Optimization of the performance indices with respect to loading and variation in the antenna structure are also examined.

The contributions of the work of this thesis include the following:

- 1) Application of interpolatory quadrature formulas to integrate the semi-infinite integrals encountered in the exact Sommerfeld formulation is illustrated.

- 2) Use of a modified method of steepest descent to evaluate the semi-infinite integrals to reduce the time of computation without significant loss of accuracy is demonstrated.
- 3) The commonly used reflection-coefficient method is derived in detail and its relative accuracy is discussed.
- 4) New, user-oriented computer programs for treating the imperfect ground problem have been developed and described.
- 5) Formulas and results convenient for application to optimization and design problems have been presented.

2. VERTICAL DIPOLES OVER THE HORIZONTAL PLANE SURFACE OF IMPERFECT GROUND

Analysis of radiation from parallel elementary vertical dipoles of the electric type, situated over a horizontal imperfect ground plane, is discussed in this chapter. First, the exact analysis of radiation from the dipoles is made using the Sommerfeld formulation. The semi-infinite integrals encountered in this formulation are evaluated numerically in an accurate way using orthogonal polynomials. For field points far away from the source points the semi-infinite integrals are evaluated using a modified saddle point method to reduce the computation time without any significant loss of accuracy. The reflection coefficient method is also derived by applying a saddle point technique to the semi-infinite integrals. Finally, a comparison of accuracy is made between the reflection coefficient method and the exact Sommerfeld formulation.

2.1. Sommerfeld Formulation

An elementary dipole of moment Idz oriented in the z -direction is located at (x', y', z') as shown in the Fig. 1. The dipole is situated over an imperfect ground plane characterized by a complex relative dielectric constant ϵ_2 . It is possible to formulate a solution to the problem of radiation from the dipole operating in the presence of the imperfect ground in terms of a single Hertzian vector π_z of the electric type. A time variation of $\exp(j\omega t)$ is assumed throughout the analysis. The Hertzian vector $\nabla_z \pi_z$ in this case satisfies the wave equation [6]

[6] A. Sommerfeld, "Partial Differential Equations in Physics," Academic Press, New York: 1964.

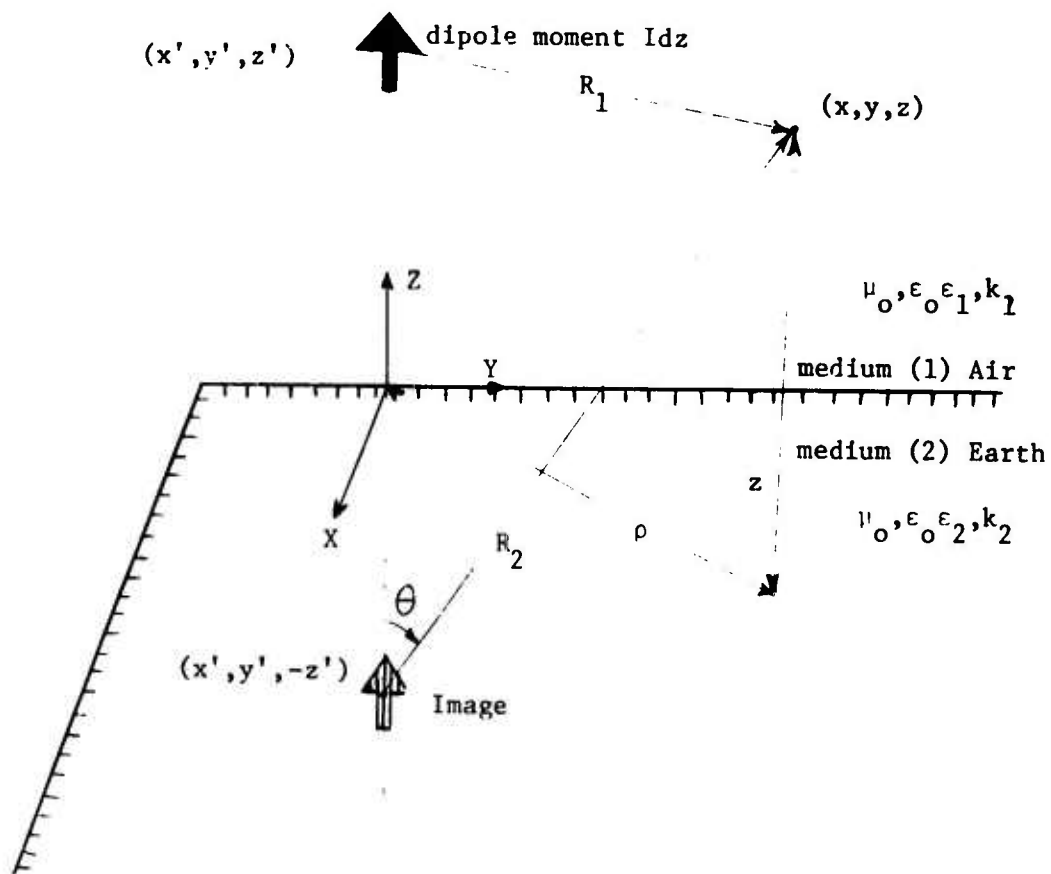


Fig. 1. Vertical dipole over a horizontal ground plane.

$$(\nabla^2 + k_1^2) V_{\pi_{1z}} = - \frac{Idz}{j\omega\epsilon_0\epsilon_1} \delta(x-x') \delta(y-y') \delta(z-z') \quad (2.1)$$

$$(\nabla^2 + k_2^2) V_{\pi_{2z}} = 0 \quad (2.2)$$

where

$$k_1^2 = \omega^2 \mu_0 \epsilon_0 \epsilon_1 \quad (2.3)$$

and

$$k_2^2 = \omega^2 \mu_0 \epsilon_0 \epsilon_2 \quad (2.4)$$

The electric and the magnetic field vectors are derived from the Hertzian vector from

$$\vec{E} = \nabla(\nabla \cdot \vec{\pi}) + k^2 \vec{\pi} \quad (2.5)$$

and

$$\vec{H} = j\omega\epsilon_0\epsilon_r (\nabla \times \vec{\pi}) \quad (2.6)$$

respectively. At the interface $z = 0$, the tangential electric and magnetic field components must be continuous, conditions which in terms of the Hertzian vector components can be written as

$$\epsilon_1 \frac{\partial \pi_{1z}}{\partial y} = \epsilon_2 \frac{\partial \pi_{2z}}{\partial y} \quad (2.7)$$

$$\epsilon_1 \frac{\partial \pi_{1z}}{\partial x} = \epsilon_2 \frac{\partial \pi_{2z}}{\partial x} \quad (2.8)$$

$$\frac{\partial}{\partial y} \left(\frac{\partial \pi_{1z}}{\partial z} \right) = \frac{\partial}{\partial y} \left(\frac{\partial \pi_{2z}}{\partial z} \right) \quad (2.9)$$

$$\frac{\partial}{\partial x} \left(\frac{\partial \pi_{1z}}{\partial z} \right) = \frac{\partial}{\partial x} \left(\frac{\partial \pi_{2z}}{\partial z} \right) \quad (2.10)$$

Since these boundary conditions must hold at $z = 0$ for all x and y , the x and y dependence of the fields on either side of the interface must be the same. Therefore,

$$\epsilon_1 \pi_{1z} = \epsilon_2 \pi_{2z} \quad [\text{from (2.7) and (2.8)}] \quad (2.11)$$

$$\frac{\partial \pi_{1z}}{\partial z} = \frac{\partial \pi_{2z}}{\partial z} \quad [\text{from (2.9) and (2.10)}] \quad (2.12)$$

The complete solutions for the Hertzian vectors satisfying the wave equations (2.1) and (2.2) and the boundary conditions (2.11) and (2.12) have been given by Sommerfeld [6], Wait [7], Miller et. al. [2] and others [8-9]. The solutions are

$$V_{\pi_{1z}} = P[\exp(-jk_1 R_1)/R_1 + \int_0^\infty \frac{J_0(\lambda \rho)}{\sqrt{\lambda^2 - k_1^2}} \frac{\epsilon_2 \sqrt{\lambda^2 - k_1^2} - \epsilon_1 \sqrt{\lambda^2 - k_2^2}}{\epsilon_2 \sqrt{\lambda^2 - k_1^2} + \epsilon_1 \sqrt{\lambda^2 - k_2^2}} \exp\{-\sqrt{\lambda^2 - k_1^2} (z+z')\} \lambda d\lambda] \quad (2.13)$$

and

$$V_{\pi_{2z}} = 2P \int_0^\infty \frac{J_0(\lambda \rho) \exp\{\sqrt{\lambda^2 - k_2^2} z - \sqrt{\lambda^2 - k_1^2} z'\}}{\epsilon_2 \sqrt{\lambda^2 - k_1^2} + \epsilon_1 \sqrt{\lambda^2 - k_2^2}} \lambda d\lambda \quad (2.14)$$

for

$$\text{Re}[\sqrt{\lambda^2 - k_{1,2}^2}] > 0. \quad \text{Here}$$

-
- [6] A. Sommerfeld, "Partial Differential Equations in Physics," Academic Press, New York, 1964.
 - [7] R. E. Collin and F. J. Zucker, "Antenna Theory: Part 2, pp. 386-437, McGraw-Hill Book Co., New York 1969.
 - [8] G. Tyras, "Radiation and Propagation of Electromagnetic Waves," Academic Press, New York, 1960.
 - [9] L. M. Brekhovskikh, "Waves in Layered Media," Academic Press, New York.

$$P = \frac{I dz}{j\omega 4\pi\epsilon_0\epsilon_1} \quad (2.15)$$

$$\rho = \sqrt{(x - x')^2 + (y - y')^2} \quad (2.16)$$

and

$$R_1 = \sqrt{\rho^2 + (z - z')^2} \quad (2.17)$$

The primed and unprimed co-ordinates are for the source and field points, respectively. For $V_{\pi_{1z}}$ the first term inside the brackets can be interpreted as the particular solution or the direct contribution from the dipole source and the second term can be interpreted as the complementary solution or a reflection term (reflection from the imperfect ground plane). Similarly the solution for $V_{\pi_{2z}}$ can be interpreted as a partial transmission of the wave from medium 1 into medium 2. With these thoughts in mind, $V_{\pi_{1z}}$ can be split up into two terms

$$V_{\pi_{1z}} = V_{\pi_{1z}}^{\text{direct}} + V_{\pi_{1z}}^{\text{refl}} = P \cdot (g_o + g_s) \quad (2.18)$$

where

$$V_{\pi_{1z}}^{\text{direct}} = P \cdot \exp(-jk_1 R_1) / R_1 \stackrel{\Delta}{=} P \cdot g_o \quad (2.19)$$

and

$$V_{\pi_{1z}}^{\text{refl}} = P \cdot \int_0^\infty \frac{\epsilon_2 \sqrt{\lambda^2 - k_1^2} - \epsilon_1 \sqrt{\lambda^2 - k_2^2}}{\epsilon_2 \sqrt{\lambda^2 - k_1^2} + \epsilon_1 \sqrt{\lambda^2 - k_2^2}} \frac{J_0(\lambda \rho) \exp[-\sqrt{\lambda^2 - k_1^2} (z + z')]}{\sqrt{\lambda^2 - k_1^2}} \lambda d\lambda \quad (2.20)$$

$$\stackrel{\Delta}{=} P \cdot g_s$$

A physical explanation to the two components of the Hertz potential $V_{\pi_{1z}}$ can be given. The first one can be explained as a spherical wave originating at the source dipole. This term is easy to deal with. The difficult problem lies in the evaluation of $V_{\pi_{1z}}^{\text{refl}}$. $V_{\pi_{1z}}^{\text{refl}}$ can be interpreted as a superposition

of plane waves resulting from reflection of the plane waves into which the original spherical wave was expanded. This arises from the identity

$$\exp(-jk_1 R_2)/R_2 = \int_0^\infty \frac{J_0(\lambda \rho) \exp[-\sqrt{\lambda^2 - k_1^2}(z + z')]}{\sqrt{\lambda^2 - k_1^2}} \lambda d\lambda \quad (2.21)$$

for $\text{Re}[\sqrt{\lambda^2 - k_1^2}] > 0$ and

$$R_2 = \sqrt{\rho^2 + (z + z')^2}. \quad (2.22)$$

The term under the integral sign of (2.21) can be recognized as plane wave decomposition of the original spherical wave source. Upon reflection of the plane waves from the dipole source as expressed in V_{1z}^{refl} , the amplitude of each wave must be multiplied by the reflection coefficient $R(\lambda)$. The complex reflection coefficient $R(\lambda)$ takes into account the phase change as the wave travels from the source (x', y', z') to the boundary and then to the point of observation (x, y, z) . The reflection coefficient $R(\lambda)$ is then defined as

$$\frac{\epsilon_2 \sqrt{\lambda^2 - k_1^2} - \epsilon_1 \sqrt{\lambda^2 - k_2^2}}{\epsilon_2 \sqrt{\lambda^2 - k_1^2} + \epsilon_1 \sqrt{\lambda^2 - k_2^2}} \quad \text{where the semi-infinite}$$

integral over $R(\lambda)$ takes into account all the possible plane waves. As $\epsilon_2 \rightarrow \infty$, g_s of (2.20) reduces to (2.21) and represents a simple spherical wave originating at the image point. This physical picture will later be applied in the derivation of the reflection coefficient method where the effect of the ground plane is approximated by modifying the components of the plane wave decomposition of the spherical wave originating from the image of the source dipole but multiplied by a specular reflection coefficient, $R(\theta)$.

There are two forms of $V_{\pi_{1z}}$ which have been used by different authors since Sommerfeld and each form has certain distinct advantages. The advantages will be presented in a later section, but the two forms used are presented here.

$$\begin{aligned}
 V_{\pi_{1z}}^{\text{refl}} &= P[\exp(-jk_1 R_2)/R_2 \\
 &\quad - 2\epsilon_1 \int_0^\infty \frac{\sqrt{\lambda^2 - k_2^2}}{\sqrt{\lambda^2 - k_1^2}} \frac{J_0(\lambda \rho) \exp[-\sqrt{\lambda^2 - k_1^2}(z+z')] }{\epsilon_2 \sqrt{\lambda^2 - k_1^2} + \epsilon_1 \sqrt{\lambda^2 - k_2^2}} \lambda d\lambda] \\
 \Delta &\equiv P[g_1 - g_{sV}]
 \end{aligned} \tag{2.23}$$

The other form is

$$\begin{aligned}
 V_{\pi_{1z}}^{\text{refl}} &= P[-\exp(-jk_1 R_2)/R_2 \\
 &\quad + 2\epsilon_2 \int_0^\infty \frac{J_0(\lambda \rho) \exp[-\sqrt{\lambda^2 - k_1^2}(z+z')]}{\epsilon_2 \sqrt{\lambda^2 - k_1^2} + \epsilon_1 \sqrt{\lambda^2 - k_2^2}} \lambda d\lambda] \\
 \Delta &\equiv P[-g_1 + g_{sV}]
 \end{aligned} \tag{2.24}$$

Both forms (2.23) and (2.24) are valid and their equivalence can be observed by applying (2.21).

2.2. Analysis of the Reflected Field

The field in the upper half space ($z > 0$) consists of the direct field from the source dipole situated at $z = z'$, its image situated at $z = -z'$, and the correction term g_{sV} used in (2.23). The correction term takes into account the nature of the imperfect ground, because as $\epsilon_2 \rightarrow \infty$, $g_{sV} \rightarrow 0$.

a) Exact Solution

The problem of determining the reflected field amounts to evaluating the integral g_{SV} since g_0 and g_1 are easy to calculate. To do this a deformed contour similar to the one suggested by Miller et. al. [2] is chosen and is indicated in Fig. 2. The deformation of the contour is possible since all the branch points and the poles lie on the second and the fourth quadrants. Hence on the deformed contour

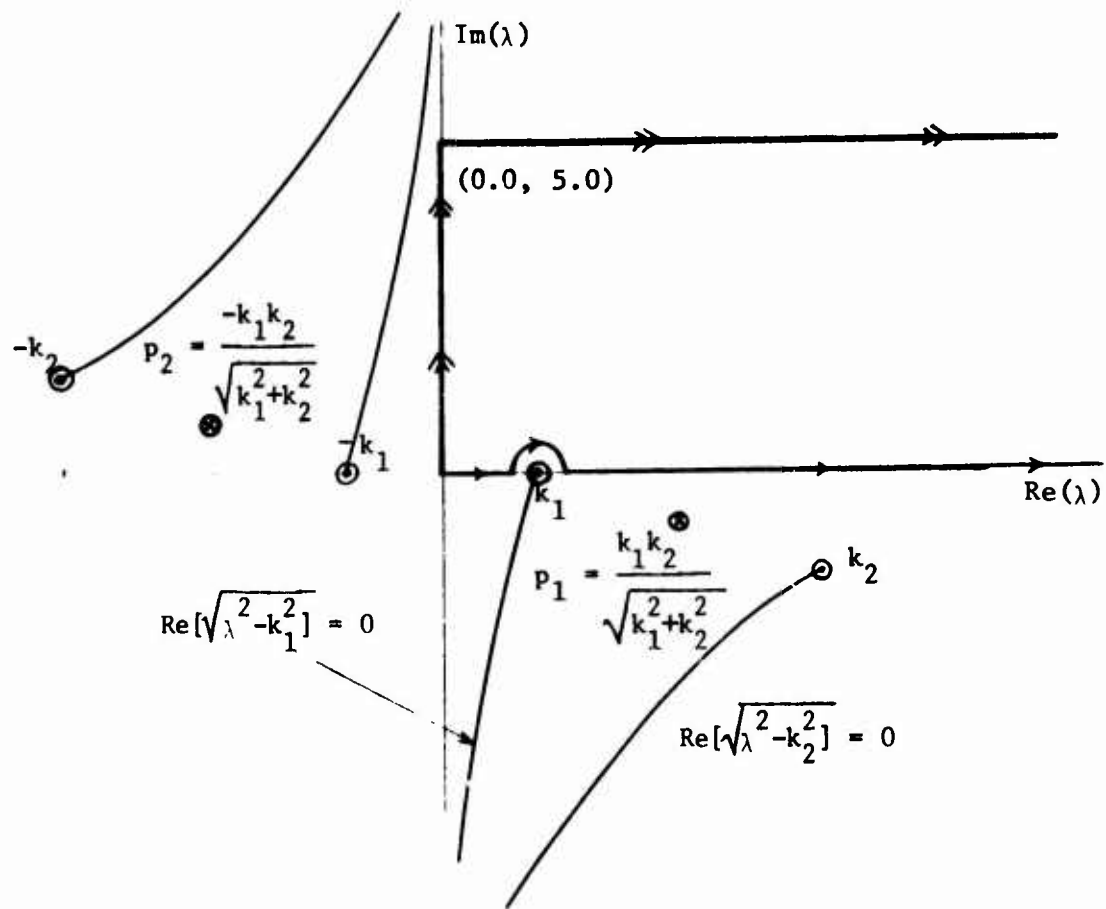
$$g_{SV} = 2j\epsilon_1 \int_0^5 \frac{I_0(\lambda\rho) \exp[-j\sqrt{\lambda^2 + k_1^2}(z + z')] \sqrt{\lambda^2 + k_2^2}}{\epsilon_2 \sqrt{\lambda^2 + k_1^2} + \epsilon_1 \sqrt{\lambda^2 + k_2^2}} \frac{\lambda d\lambda}{\sqrt{\lambda^2 + k_1^2}} \\ + 2\epsilon_1 \int_0^\infty \frac{J_0(\beta\rho) \exp[-\sqrt{\beta^2 - k_1^2}(z + z')] \sqrt{\beta^2 - k_2^2}}{\epsilon_2 \sqrt{\beta^2 - k_1^2} + \epsilon_1 \sqrt{\beta^2 - k_2^2}} \frac{\beta d\lambda}{\sqrt{\beta^2 - k_1^2}} \quad (2.25)$$

where $\beta = \lambda + j5$. The judicious choice of 5 as the limit of the first

integral is made, because then the poles of g_{SV} at $\pm \frac{k_1 k_2}{\sqrt{k_1^2 + k_2^2}}$ have

negligible effect on the numerical evaluation of the integral. The modified Bessel function of the first kind in the first integral and the Bessel function of a complex argument in the second integral are computed by [10, 11]. Finally the two integrals are computed by using the Gaussian interpolatory quadrature and the Gaussian Laguerre interpolatory quadrature formulas, respectively. A description of the method is discussed in Appendix A.

-
- [10] T. K. Sarkar and J. E. Lewis, "Accurate Generation of Real Order and Argument Bessel and Modified Bessel Functions," Proc. IEE, p. 34, January 1973.
 - [11] J. E. Lewis, T. K. Sarkar and P. D. O'Kelley, "Generation of Bessel Functions of Complex Order and Argument," Electron. Lett., vol. 7, No. 20, pp. 615-616.



- \otimes - poles
- \odot - branch points
- \rightarrow - contour of integration
- \rightarrow - modified contour

Fig. 2. Contour of integration in the complex λ plane.

It was because of these methods it was possible to evaluate these integrals in reasonable time.

The major problem of this technique is that for large values of ρ , the values of the integrals in (2.25) are quite large and they have to be subtracted from each other to yield a relatively small value. This could be observed from the behavior of $I_0(\lambda\rho)$, since it is a monotonically increasing function of ρ . However this formulation is quite useful for small values of ρ .

b) Reflection Coefficient Method:

For large values of ρ the method of steepest descent is applied to analyze the fields of the reflected wave at distances far from the source. Under this circumstance, it is convenient to use an infinite integral representation of g_{SV} rather than the semi-infinite integral representation. Use of

$$J_n(x) = \frac{1}{2}[H_n^{(1)}(x) + H_n^{(2)}(x)] \quad (2.26)$$

and

$$H_n^{(1)}(xe^{j\pi}) = -e^{-jn\pi} H_n^{(2)}(x) \quad (2.27)$$

in (2.23) expresses g_{SV} as

$$g_{SV} = -jc_1 \int_C \frac{\sqrt{k_2^2 - \lambda^2}}{\sqrt{k_1^2 - \lambda^2}} \frac{H_0^{(2)}(\lambda\rho) \exp[-j\sqrt{k_1^2 - \lambda^2}(z + z')]}{\epsilon_2 \sqrt{k_1^2 - \lambda^2} + \epsilon_1 \sqrt{k_2^2 - \lambda^2}} \lambda d\lambda \quad (2.28)$$

where C is a contour as shown by Fig. 3. g_{SV} is now a spectrum of plane waves travelling away from the ground plane with the vertical component of the propagation constant as $\sqrt{k_1^2 - \lambda^2}$. The integral in (2.28) contains double valued functions $\sqrt{k_{1,2}^2 - \lambda^2}$. The proper sheet of the double valued functions are those on which the radiation condition [12] is satisfied, [12] Ref. [6], p. 189.

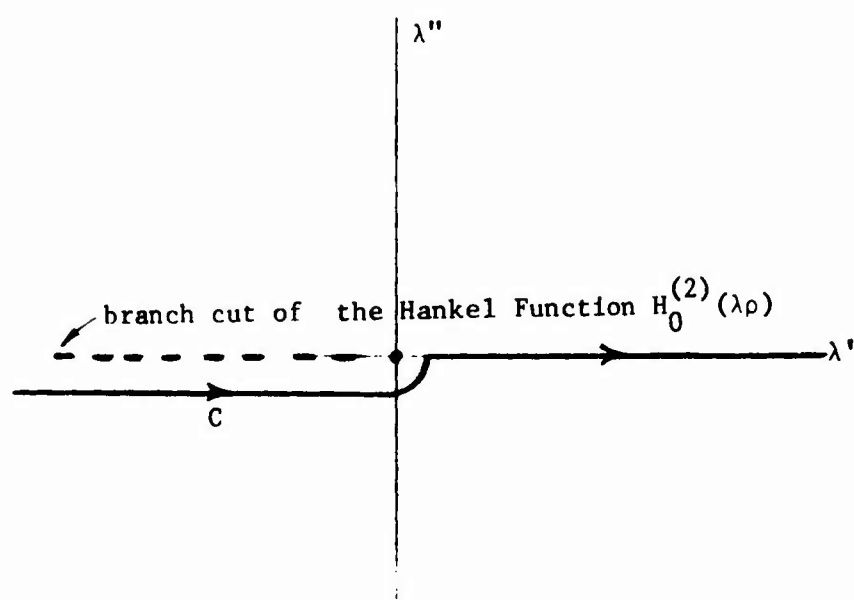


Fig. 3. Path of integration for g_{8V} .

i.e. $g_{SV} \rightarrow 0$ as $\rho \rightarrow \infty$ for a fixed z , and $g_{SV} \rightarrow 0$ as $z \rightarrow \infty$ for a fixed ρ .

Since

$$H_0^{(2)}(\lambda\rho) \xrightarrow{|\lambda\rho| \rightarrow \infty} \frac{2}{\sqrt{\pi\lambda\rho}} \exp[-j(\lambda\rho - \pi/4)] \quad (2.29)$$

the convergence of (2.28) is assured when $\text{Im}(\lambda) \leq 0$ as $\rho \rightarrow \infty$. Convergence is also assured for

$$\text{Im}(k_1^2 - \lambda^2)^{1/2} < 0 \quad \text{as } z \rightarrow \infty, \quad (2.30)$$

and for

$$(k_1^2 - \lambda^2)^{1/2} \xrightarrow{\lambda \rightarrow 0} k_1' + jk_1'', \quad k_1' > 0, \quad k_1'' \leq 0. \quad (2.31)$$

If

$$(k_1^2 - \lambda^2)^{1/2} = \tau' + j\tau'' \quad (2.32)$$

then

$$\tau'' = \frac{k_1' k_1'' - \lambda' \lambda''}{\tau'} \quad (2.33)$$

and

$$\tau' = \left\{ \left[\frac{k_1'^2 - k_1''^2 - \lambda'^2 + \lambda''^2}{2} \right]^2 + (k_1' k_1'' - \lambda' \lambda'')^2 \right\}^{1/2} + \frac{k_1'^2 - k_1''^2 - \lambda'^2 + \lambda''^2}{2} \quad (2.34)$$

where

$$\lambda = \lambda' + j\lambda'' \triangleq \text{Re}(\lambda) + j \text{Im}(\lambda) \quad (2.35)$$

The positive sign is chosen for τ' since $\tau' > 0$ (from (2.31)). On the path of integration $\tau'' < 0$ and if $k_1'' \neq 0$, then convergence would be assured even if $\lambda'' = 0$. If medium 1 is lossless $k_1'' = 0$ then from (2.33) $\lambda' > 0$ when $\lambda'' > 0$ and $\lambda' < 0$ when $\lambda'' < 0$. The first condition $\lambda'' > 0$ conflicts with the convergence requirement for the Hankel function $H_0^{(2)}(\lambda\rho)$. This problem can be avoided if medium 1 is assumed to be lossy (i.e., $k_1'' \neq 0$) and the "lossless case" then assumed to be the limiting form of the expression $k_1'' \rightarrow 0$. Since $H_0^{(2)}(\lambda\rho)$ can be integrated through the origin

($\lambda = 0$) even if $\lambda'' = 0$, the path C of Fig. 3 can be modified to the path C_1 of Fig. 4, following the real axis from $-\infty$ to $+\infty$.

The integral in (2.28) can be simplified by making the following substitutions:

$$\lambda = k_1 \sin \beta \quad (2.36)$$

$$\rho = R_2 \sin \theta \quad (2.37)$$

$$z + z' = R_2 \cos \theta \quad (2.38)$$

The interpretation of the angle θ is shown in Fig. 1. Hence by the application of (2.29), (2.36), (2.37) and (2.38) to (2.28) yields

$$g_{SV} \approx \int_{\Gamma_1} \left[\frac{2k_1 \sin \beta}{\pi R_2 \sin \theta} \right]^{1/2} \frac{\sqrt{\epsilon - \sin^2 \beta}}{\epsilon \cos \beta + \sqrt{\epsilon - \sin^2 \beta}} \exp[j\{-\pi/4 - k_1 R_2 \cos(\beta - \theta)\}] d\beta \quad (2.39)$$

where $\epsilon = \epsilon_2/\epsilon_1$ and Γ_1 is a path in the complex β plane as shown in Fig. 5.

There is one obvious weakness in the arguments presented to derive (2.39), namely, that there are points on the path for which the argument of the Hankel function $H_0^{(2)}(\lambda\rho)$ used in (2.29), is not large and may even be zero, so that the asymptotic expansion for large arguments cannot be used. However as argued by Brekhovskikh [9], the arguments will be rigorous if the large argument approximation is used only after the path of integration has been changed to the path of steepest descent Γ_0 . The result will then be the same.

Assuming medium 1 to be lossless, so that k_1 is real, the transformation $\lambda = k_1 \sin \beta$ implies ($\beta = \beta' + j\beta''$)

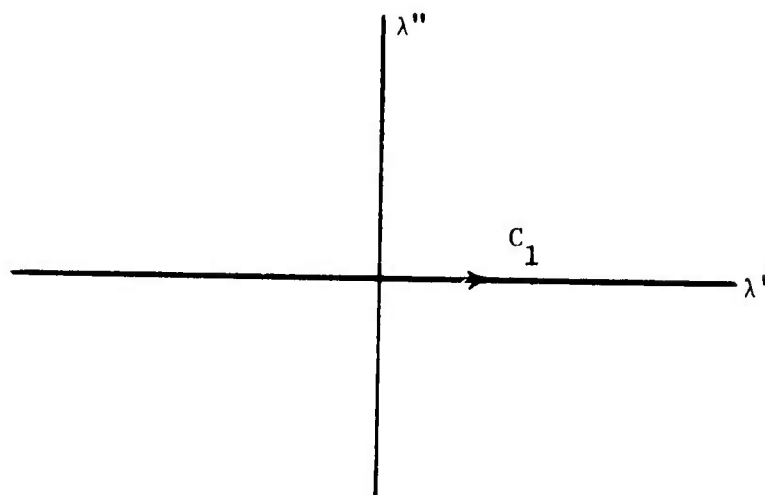


Fig. 4. Modified path of integration for g_{SV} .

$$\lambda' + j\lambda'' = k_1(\sin \beta' \cosh \beta'' + j \cos \beta' \sinh \beta'') \quad (2.40)$$

or

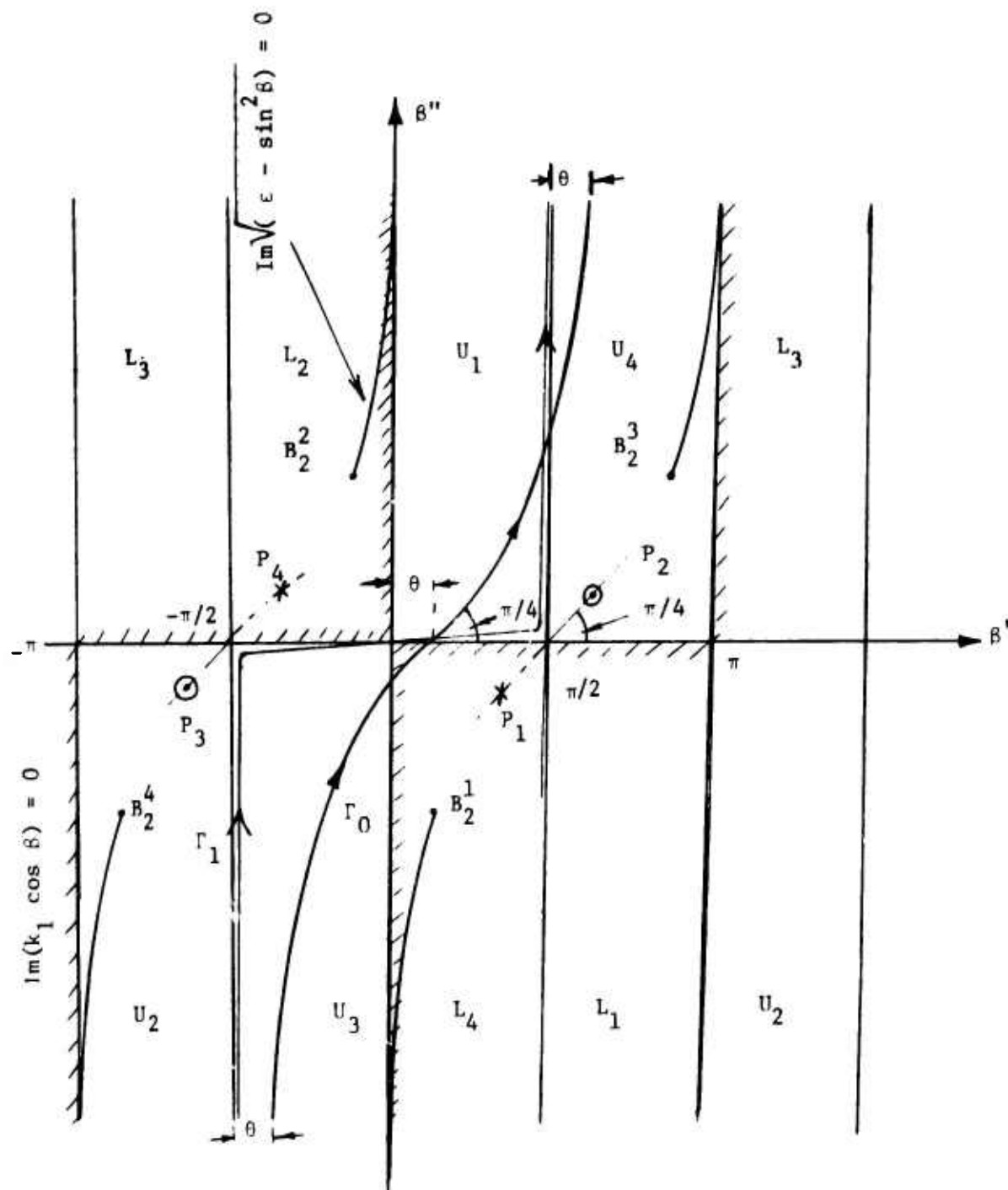
$$\lambda' = k_1 \sin \beta' \cosh \beta'' \quad (2.41)$$

$$\lambda'' = k_1 \cos \beta' \sinh \beta'' . \quad (2.42)$$

Hence the mapping transforms the quadrants of the λ -plane in parallel strips of width $\pi/2$ radians, and the path of integration from $\lambda' = -\infty$ to ∞ is transformed to the path Γ_1 , where $\lambda'' = \text{Im}(k_1 \sin \beta) = 0$, as shown in Fig. 5. The requirement $\text{Im}(\sqrt{k_1^2 - \lambda^2}) < 0$ amount to $\text{Im}(k_1 \cos \beta) < 0$ on the path of integration, or for k_1 real $\sin \beta' \sinh \beta'' > 0$. The script 'U' denotes the strips of the β -plane on which the above inequality is satisfied (upper Riemann sheet) and the others by 'L' (lower Riemann Sheet). The path Γ_1 then totally lies on U. The location of the branch points at $\lambda = \pm k_1$ in the λ -plane are now transformed into $\sin \beta_{B_1} = \pm k_1$ in the β -plane and are situated at $\pm \pi/2, \pm 3\pi/2$ and so on. The branch cuts $\text{Im}(\sqrt{k_1^2 - \lambda^2}) = 0$ are now transformed to $\text{Im}(k_1 \cos \beta) = 0$, and begin at the branch points β_{B_1} . Since $\text{Im}(k_1 \cos \beta) = \text{Im}[k_1 \sin(\pi/2 \pm \beta)]$, these branch cuts will run parallel to the path Γ_1 , [$\text{Im}(k_1 \sin \beta) = \lambda'' = 0$] but shifted by $\pm \pi/2$ along the real axis. So the transformation $\lambda = k_1 \sin \beta$ has transformed the upper and lower sheets associated with the branch points $\pm k_1$ into one sheet where certain strips on the sheet belong to the previous upper (U) and lower (L) Riemann sheet on the λ -plane.

The remaining branch points $\lambda = \pm k_2$ are transformed to $\sin \beta_{B_2} = \pm \sqrt{\epsilon_2/\epsilon_1} = \pm \sqrt{\epsilon}$ which has solutions

$$\beta_{B_2} = j \ln[\pm j\sqrt{\epsilon} \pm \sqrt{1 - \epsilon}]. \quad (2.43)$$



$\text{Im}(k_1 \cos \beta) < 0$ inside the shaded region.

Fig. 5. The complex β -plane showing possible branch points, branch cuts, poles and the path of steepest descent for $\epsilon = \epsilon'(1-j)^2$ and $|\epsilon| \gg 1$.

The branch cuts $\text{Im}[(k_2^2 - \lambda^2)^{1/2}] = 0$ are transformed into $\text{Im}[(\epsilon_2 - \epsilon_1 \sin \beta)^{1/2}] = \text{Im}[(\epsilon - \sin \beta)^{1/2}] = 0$. In the β -plane there are then two Riemann sheets connected along the branch cuts $\text{Im}[(\epsilon - \sin \beta)^{1/2}] = 0$ of the branch points β_{B_2} . Finally the poles in the λ -plane are now given by

$$\sin \beta_P = \pm \sqrt{\frac{\epsilon}{1 + \epsilon}} \quad (2.44)$$

The case for which $\epsilon = \epsilon'(1-j)^2$ is of interest since this is a good approximation of the complex refractive index of both earth and sea water over a wide range of frequencies. The displacement current is negligible in comparison to the conduction current if the frequencies are limited below about 1MHz. For a special case $\epsilon = \epsilon'(1-j)^2$ and $\|\epsilon\| \gg 1$, the locations of the branch points β_{B_2} and the poles β_P can be approximated by

$$\beta_{B_2}^{1,2} = \pm \pi/4 \mp j \ln(\sqrt{8\epsilon'})$$

$$\beta_{B_2}^{3,4} = \pm 3\pi/4 \pm j \ln(\sqrt{8\epsilon'})$$

$$P_{1,2} = [\pi/2 \mp 1/(2\sqrt{\epsilon'})] \mp \frac{j}{2\sqrt{\epsilon'}}$$

$$P_{2,3} = -(\pi/2 \mp \frac{1}{2\sqrt{\epsilon'}}) \mp \frac{j}{2\sqrt{\epsilon'}}$$

and they are illustrated in Fig. 5. Out of the possible locations of the branch points and poles only $\beta_{B_2}^2, \beta_{B_2}^3, P_2$ and P_3 are situated on the upper Riemann sheet of branch points β_{B_2} on which $\text{Im}(k_1 \cos \beta) < 0$. It is also important to note that none of the poles (P_2, P_3) are situated between the original path of integration Γ_1 and the path of steepest descent Γ_0 . For

this particular case $\epsilon = \epsilon'(1-j)^2$ the poles P_1 and P_2 are on a line having a slope $\pi/4$ with respect to the β' axis. The path of steepest descent also makes an angle $\pi/4$ and it increases as it goes up in U_4 plane. Hence the pole will never be intercepted by the path of steepest descent. However when the path of steepest descent Γ_0 lies in close proximity of the pole P_2 , special precautions must be taken in the evaluation of the integral of (2.39). The pole P_1 is of no concern since it lies on the second Riemann sheet of the branch point β_{B_2} on which $\text{Im}(\sqrt{\epsilon - \sin^2 \beta}) > 0$. The presence of the branch point B_3 should ordinarily be taken into account while deforming the path Γ_1 to the path of steepest descent Γ_0 . The location of the branch point is such that its imaginary part is proportional to $\ln(\sqrt{8\epsilon'})$, which for large ϵ is very large. Because of this reason, as explained by Tyras [8], the contribution along the borders of the branch cut would be a fast decreasing exponential that can be neglected in comparison to the contribution from the saddle point integration.

For $\theta < \pi/2$, application of (B.2) and (B.4) to (2.39) yields

$$g_{sv} \approx \frac{2 \exp(-jk_1 R_2)}{R_2} \frac{\sqrt{\epsilon - \sin^2 \theta}}{\epsilon \cos \theta + \sqrt{\epsilon - \sin^2 \theta}} \times$$

$$\left[1 - \frac{1}{2jk_1 R_2} \left\{ \frac{\epsilon(\epsilon-1)[2\epsilon(\epsilon-1) + \epsilon \cos^2 \theta (3 - \cos^2 \theta) + \cos \theta \sqrt{\epsilon - \sin^2 \theta} (2\epsilon + \sin^2 \theta)]}{(\epsilon - \sin^2 \theta)^2 [\epsilon \cos \theta + \sqrt{\epsilon - \sin^2 \theta}]^2} - \frac{1}{4 \sin^2 \theta} \right\} \right]$$

(2.45)

$v_{\pi_{1z}}^{\text{refl}}$ is obtained from (2.23) as,

$$\begin{aligned}
V_{\pi_{1z}}^{\text{refl}} \approx P \cdot \frac{\exp(-jk_1 R_2)}{R_2} & \left[\frac{\epsilon \cos \theta - \sqrt{\epsilon - \sin^2 \theta}}{\epsilon \cos \theta + \sqrt{\epsilon - \sin^2 \theta}} \right. \\
+ \frac{1}{jk_1 R_2} & \left\{ \frac{\epsilon(\epsilon-1)[2\epsilon(\epsilon-1) + \epsilon \cos^2 \theta (3 - \cos^2 \theta) + \cos \theta (2\epsilon + \sin^2 \theta) \sqrt{\epsilon - \sin^2 \theta}]}{(\epsilon - \sin^2 \theta)^{3/2} [\epsilon \cos \theta + \sqrt{\epsilon - \sin^2 \theta}]^3} \right. \\
& \left. \left. - \frac{\sqrt{\epsilon - \sin^2 \theta}}{2 \sin^2 \theta [\epsilon \cos \theta + \sqrt{\epsilon - \sin^2 \theta}]} \right\} \right] \quad (2.46)
\end{aligned}$$

For very low dielectric constant this method would be inaccurate as then the contribution from the branch cut connecting B_2^3 to $(\pi + j\infty)$ would have to be taken into account and the second terms of (2.45) and (2.46) would be different.

The first term of (2.46) which has a spherical wave representation of the original source but now emanating from its image can then be represented as

$$V_{\pi_{1z}}^{\text{refl}} \approx P \cdot \Gamma_{\text{TM}} \exp(-jk_1 R_2) / R_2 \quad (2.47)$$

where Γ_{TM} can be recognized as the specular plane wave TM reflection coefficient [13], given by

$$\Gamma_{\text{TM}} = \frac{\epsilon \cos \theta - \sqrt{\epsilon - \sin^2 \theta}}{\epsilon \cos \theta + \sqrt{\epsilon - \sin^2 \theta}} \quad (2.48)$$

The name "Reflection Coefficient Method" derives from (2.47) since $V_{\pi_{1z}}^{\text{refl}}$ is now obtained as the reflection coefficient times the potential from the image of the source. This method represents a good approximation, as long as the fields are computed far away from the source and away from the imperfect ground plane to ensure $\theta < \pi/2$. The far fields due to the reflected ray are given by [14]

[13] E. C. Jordan and K. G. Balmain, "Electromagnetic Waves and Radiating Systems," pp. 628-654, Prentice Hall, New Jersey, 1968.

[14] R. F. Harrington, "Time Harmonic Electromagnetic Fields," McGraw-Hill, New York 1961, p. 133.

$$E_{\rho}^{\text{refl}} = j\omega\mu_0 \sin \theta \cos \theta P \cdot V_{\pi_{1z}}^{\text{refl}}$$

and

$$E_z^{\text{refl}} = -j\omega\mu_0 \sin^2 \theta P \cdot V_{\pi_{1z}}^{\text{refl}}$$

or

$$E_{\rho}^{\text{refl}} = j\omega\mu_0 \sin \theta \cos \theta P \cdot \Gamma_{\text{TM}} \exp(-jk_1 R_2)/R_2$$

$$= \Gamma_{\text{TM}} \times (\text{far field from the image}) \quad (2.49)$$

and

$$E_z^{\text{refl}} = -j\omega\mu_0 \sin^2 \theta P \cdot \Gamma_{\text{TM}} \exp[-jk_1 R_2]/R_2$$

$$= \Gamma_{\text{TM}} \times (\text{far field from the image}) \quad (2.50)$$

The direction and the position of the image in (2.49) and (2.50) is given by considering the same dipole now situated over a perfect ground plane. A physical explanation can now be given for (2.49) and (2.50). A plane of incidence is now defined as a plane containing both the vertical dipole and the field point but perpendicular to the ground plane. Then the contribution of the reflected ray in this plane is obtained by multiplying E_{ρ} and E_z (defined in this plane) by the specular TM reflection coefficient. This is different from the exact solution of (2.20) in that now instead of infinitely many waves, each multiplied by a reflection coefficient $R(\lambda)$, all the plane waves are multiplied by the specular reflection coefficient $R(\theta)$.

When the conductivity of the earth is large, $|\epsilon| \gg 1$, the Hertz potential in medium (1) is then obtained from (2.18), (2.19) and (2.45)

$$V_{\pi_{1z}} = P[\exp(-jk_1 R_1)/R_1 + \exp(-jk_1 R_2)/R_2 \times \\ \{ \frac{\sqrt{\epsilon} \cos \theta - 1}{\sqrt{\epsilon} \cos \theta + 1} + \frac{2\epsilon}{jk_1 R_2} (\frac{1}{\sqrt{\epsilon} \cos \theta + 1})^3 + \dots \}]$$

Note that when $|\epsilon| \rightarrow \infty$, $V_{\pi_{1z}}$ goes properly into the form of a field due to a vertical electric dipole above a perfectly conducting ground plane. However when $\theta \sim \pi/2$

$$V_{\pi_{1z}} = P[\exp(-jk_1 R_1)/R_1 - \exp(-jk_1 R_2)/R_2 + \frac{2\epsilon}{jk_1 R_2} \exp(-jk_1 R_2) + \dots] \quad (2.51)$$

The sum of the first two terms may be smaller than the third term. As a matter of fact, when both the transmitter and the receiver are on the ground, $R_1 = R_2 = \rho$, and $z = 0 = z'$, the fields will be solely determined by the second and higher order terms. The reason for poor convergence in the vicinity of $\theta = \pi/2$ is that the effect of the pole at $\pi/2$ becomes important. This has been taken into account in the formulation of the problem in the next section.

c) Fields Near the Interface

In order to solve for the fields near the interface a modified saddle point method as explained in Appendix B is applied to take into account the pole near the saddle point. The expression for g_{zy} in (2.39) has a pole β_p , which is obtained from $\epsilon \cos \beta_p + \sqrt{\epsilon - \sin^2 \beta_p} = 0$.

Hence

$$\sin \beta_p = \sqrt{\frac{\epsilon}{\epsilon + 1}} \quad (2.52)$$

and

$$\cos \beta_p = -\sqrt{\frac{1}{\epsilon + 1}} \quad (2.53)$$

The positive sign in front of the square root in (2.53) is inadmissible because then

$$\text{Im}(\sqrt{\epsilon - \sin^2 \beta_p}) = \text{Im}(-\epsilon \cos \beta_p) = -\text{Im}\left[\frac{\epsilon}{\sqrt{\epsilon+1}}\right] > 0 \text{ (since } \epsilon = \epsilon' - j\epsilon'').$$

Hence from (B.5), (B.6) and (B.10)

$$\begin{aligned} g_{SV} &\approx \exp[-j\pi/4] \left(\frac{2k_1}{\pi R_2}\right)^{1/2} \frac{\sqrt{\epsilon - \sin^2 \theta}}{\epsilon^2 - 1} \frac{\sqrt{\epsilon - \sin^2 \theta - \epsilon \cos \theta}}{\cos \theta - 1/\sqrt{\epsilon+1}} \times \\ &\quad \frac{1}{2 \sin(\frac{\theta + \beta_p}{2})} \int_{\Gamma_1} \frac{\exp[-jk_1 R_2 \cos(\beta - \theta)]}{\sin(\frac{\beta - \beta_p}{2})} d\beta \\ &\approx \left(\frac{4\pi k_1 j}{R_2}\right)^{1/2} \frac{\sqrt{\epsilon - \sin^2 \theta}}{\epsilon^2 - 1} \frac{\sqrt{\epsilon - \sin^2 \theta - \epsilon \cos \theta}}{\cos \theta - 1/\sqrt{\epsilon+1}} \\ &\quad \times \frac{\exp[-jk_1 R_2 - W^2] \text{erfc}(jW)}{\left\{1 + \frac{\cos \theta}{\sqrt{\epsilon+1}} + \frac{\sqrt{\epsilon} \sin \theta}{\sqrt{\epsilon+1}}\right\}^{1/2}} \end{aligned} \quad (2.54)$$

where

$$\begin{aligned} W^2 &= -jk_1 R_2 \times 2 \times \sin^2\left(\frac{\theta - \beta_p}{2}\right) \\ &= -jk_1 R_2 \left[1 + \frac{\cos \theta}{\sqrt{\epsilon+1}} - \frac{\sqrt{\epsilon} \sin \theta}{\sqrt{\epsilon+1}}\right] \end{aligned} \quad (2.55)$$

V_{1z}^{refl} can now be obtained after g_{SV} is obtained from (2.54). This method then can be applied to calculate the Hertz potential for large ρ since the exact solution described in part (a) of this section becomes inaccurate. This method is used to compute V_{1z} for a choice of $\rho \geq 0.5\lambda$. The primary source of error in using this formula for a source ($x' = 0, y' = 0, z' = 0.25\lambda$) and a field point ($x = 0, y = 0.5\lambda, z = 0.25\lambda$)

would be the error in representing $H_0^{(2)}(k_1 \rho \sin \theta)$ by its large argument approximation assuming the higher order terms in the saddle point method are negligible compared to the first term. For this case the error in representing $H_0^{(2)}(\pi/\sqrt{2})$ by its large argument approximation is one percent in magnitude and -3° in phase. But after we would be interested in antenna arrays closer to the ground plane than 0.25λ . Hence the error would always be less than the upper bound presented.

The quantity W presented in (2.55) is known as the numerical distance in the literature. When $|\epsilon|$ is large

$$W^2 \approx - \frac{j k_1 R_2}{2\epsilon} [1 + (\pi/2 - \theta) \sqrt{\epsilon}]^2, \quad (2.56)$$

The modulus of the numerical distance W can be of the order of unity or less, in spite of the fact that $k_1 R_2$ is large. It is thus evident that the condition $|W^2| \gg 1$ can turn out to be considerably more rigid than the condition $k_1 R_2 \gg 1$. Different approximations used for the Hertz potentials mentioned by various authors [4,5] in literature are generally valid for $|W| \gg 1$ except for Banos [1]. Sommerfeld [6] gives a very interesting physical interpretation of numerical distance. It is the difference in phase shifts $k_1 \rho$ and $k_s \rho$ of a spatial wave and a surface wave respectively, where $k_s^2 = \frac{k_1^2 k_2^2}{k_1^2 + k_2^2}$. Sommerfeld thus defines the numerical distance W_1 to be $W_1 = -j(k_1 - k_s)\rho$. The absolute value of W_1 is small compared to $k_1 \rho$. In fact for large $|\epsilon|$

$$|W_1| \approx \frac{k_1 \rho}{2} \frac{k_1^2}{|k_2|^2} = \frac{k_1 \rho}{2|\epsilon|} \quad (2.57)$$

For small values of $|W_1|$ the spatial wave type (due to g_0 and g_1) predominates in the expression of the reception intensity. In this case, the ground constants have no marked influence. For larger $|W_1|$, the relations between the spatial and surface waves (due to g_{sv}) becomes important. In this case the complex ground dielectric constant ϵ_2 has a marked influence. When both the transmitter and the receiver are on the ground, i.e. $\theta \approx \pi/2$ then $|W^2| = |W_1|$ from (2.55 and 2.57). For $\theta \approx \pi/2$ and $|W| \approx 1$, the disadvantage associated with the representation of $V_{\pi_{1z}}^{\text{refl}}$ by (2.23) is that the second and higher order terms in the modified saddle point evaluation of g_{sv} cannot be neglected. Even though formulas exist for generating higher order terms, the procedure is very tedious since it involves taking higher-order derivatives of the integrand.

The reason for using (2.24) now becomes clear. When the dipole and the observation point are both at the interface, the first two terms g_0 and g_1 of $V_{\pi_{1z}}$ in (2.24) tends to cancel each other and the field is solely determined by the integral of G_{sv} , just by the leading term of the asymptotic expansion of G_{sv} . Substitution of (2.29), (2.36), (2.37) and (2.38) in the expression G_{sv} in (2.24) and application of the modified method of steepest descent as of (B.5) and (B.10) yields,

$$\begin{aligned}
G_{SV} &\approx \epsilon \exp(-j\pi/4) \int_0^{\pi/2} \left(\frac{2k_1 \sin \beta}{\pi R_2 \sin \theta} \right)^{1/2} \frac{\cos \beta}{\epsilon \cos \beta + \sqrt{\epsilon - \sin^2 \beta}} \times \\
&\quad \exp[-jk_1 R_2 \cos(\beta - \theta)] d\beta \\
&\approx \epsilon \left(\frac{4\pi k_1 j}{R_2} \right)^{1/2} \frac{\cos \theta}{\cos \theta - 1/\sqrt{\epsilon + 1}} \frac{\sqrt{\epsilon - \sin^2 \theta} - \epsilon \cos \theta}{\epsilon^2 - 1} \\
&\quad \times \frac{\exp[-jk_1 R_2 - W^2] \operatorname{erfc}(jW)}{\left\{ 1 + \frac{\cos \theta}{\sqrt{\epsilon + 1}} + \frac{\sqrt{\epsilon} \sin \theta}{\sqrt{\epsilon + 1}} \right\}^{1/2}} \quad (2.58)
\end{aligned}$$

where W^2 is given by (2.55).

Hence for $|W| > 1$ or $k_1 R_2 > |\epsilon|$, the second form of $V_{\pi_{1z}}^{\text{refl}}$ as given by (2.24) is used to compute the Hertz Potential.

2.3. Evaluation of Mutual Impedance between two Parallel Vertical Dipoles Situated over a Plane Imperfect Ground

In this section, an expression is obtained for the mutual impedance between two z-directed current elements of lengths ℓ_A and ℓ_B carrying a current distribution I_A and I_B , situated over a horizontal imperfect ground plane. The corresponding configuration is presented in Fig. 6. The electric field \vec{E}_A in medium 1 from the current element I_A is given by (2.5)

$$\begin{aligned}
\vec{E}_A &= \{k_1^2 + \vec{\nabla} \frac{\partial}{\partial z}\} V_{\pi_{1z}} \quad (\text{replacing } V_{\pi_{1z}} \text{ by 2.18}) \\
&= -\frac{j\omega\mu_0}{4\pi} \int_{\ell_A} z I_A (g_o + g_s) dz'_A \\
&\quad + \frac{\vec{\nabla}}{j\omega 4\pi\epsilon_0} \frac{\partial}{\partial z} \int I_A (g_o + g_s) dz'_A \quad (2.59)
\end{aligned}$$

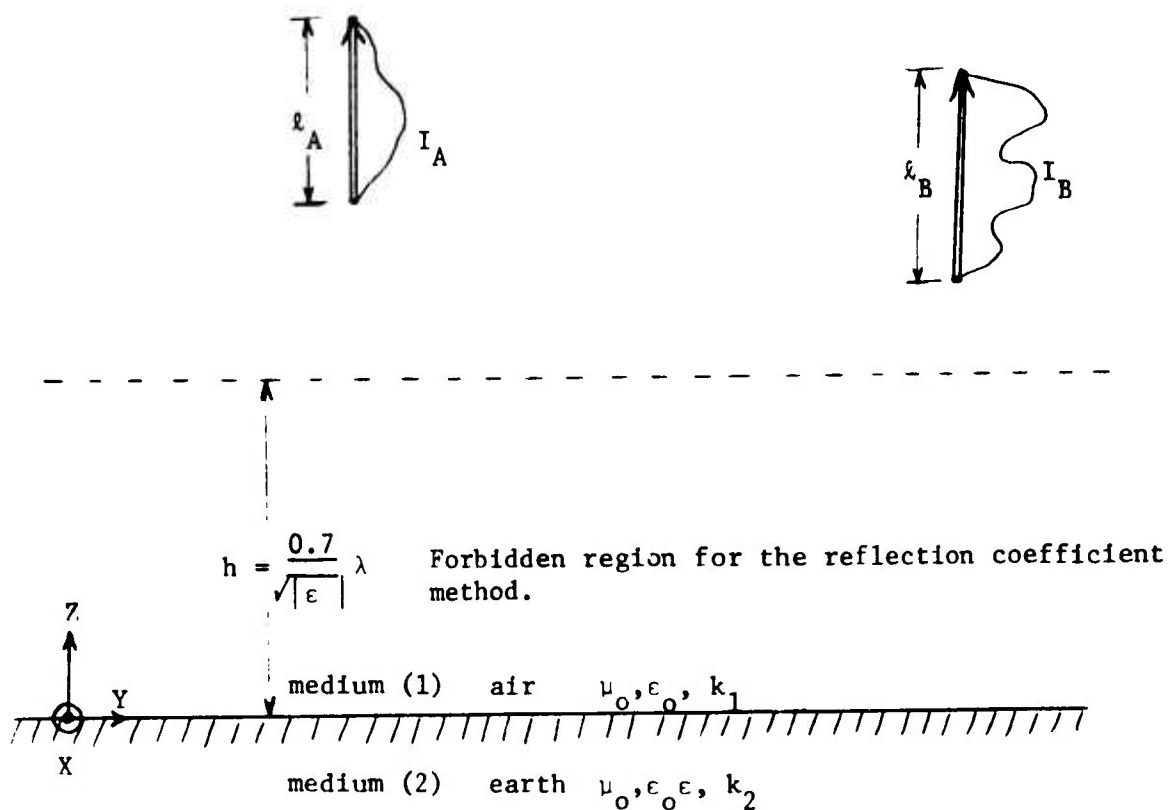


Fig. 6. Two parallel z-directed vertical dipoles of lengths l_A and l_B having a current distribution of I_A and I_B situated over a horizontal earth.

Since $\frac{\partial g_o}{\partial z} = - \frac{\partial g_o}{\partial z'_A}$ and $\frac{\partial g_s}{\partial z} = \frac{\partial g_s}{\partial z'_A}$, and

assuming the current I_A goes to zero at the ends of the open wires, the derivative $(\frac{\partial}{\partial z})$ operation on $(g_o + g_s)$ can be transferred to $\frac{\partial}{\partial z'_A}$

now operating on I_A instead. Hence

$$\vec{E}_A = - \frac{j\omega\mu_o}{4\pi} \int_{\ell_A} 2 I_A (g_o + g_s) dz'_A + \frac{\vec{\nabla}}{j\omega 4\pi\epsilon_o} \int_{\ell_A} \frac{dI_A}{dz'_A} (g_o - g_s) dz'_A \quad (2.60)$$

The mutual impedance Z_{BA} between two z-directed current elements I_A and I_B is expressed as

$$\begin{aligned} Z_{BA} &= - \int_{\ell_B} \vec{E}_A \cdot \vec{I}_B dz'_B \\ &= \frac{j\omega\mu_o}{4\pi} \int_{\ell_B} I_B dz'_B \int_{\ell_A} I_A (g_o + g_s) dz'_A \\ &\quad - \frac{1}{j\omega 4\pi\epsilon_o} \int_{\ell_B} I_B \frac{\partial}{\partial z'_B} \left\{ \int_{\ell_A} \frac{dI_A}{dz'_A} (g_o - g_s) dz'_A \right\} dz'_B \end{aligned} \quad (2.61)$$

Transferring the derivative operation on I_B in the second term and assuming I_B goes to zero at open ends of the wires

$$\begin{aligned} Z_{BA} &= \frac{j\omega\mu_o}{4\pi} \int_{\ell_B} I_B dz'_B \int_{\ell_A} I_A (g_o + g_s) dz'_A \\ &\quad + \frac{1}{j\omega 4\pi\epsilon_o} \int_{\ell_B} \frac{dI_B}{dz'_B} dz'_B \int_{\ell_A} \frac{dI_A}{dz'_A} (g_o - g_s) dz'_A \end{aligned} \quad (2.62)$$

If a piecewise sinusoidal current distribution is assumed for I_A and I_B the integrals over l_A and l_B can be performed analytically. But this introduces a third order pole at the origin of the semi-infinite integrals defined for g_s . Hence a four pulse approximation to the piecewise linear (triangle) function [15] is used. In this case also, the double integrals in (2.62) can be evaluated analytically, leaving only the semi-infinite integral to be evaluated numerically.

For the computation of the self impedance Z_{AA} , ρ in (2.62) is replaced by the radius of the wire antenna.

The numerical value of the mutual impedance Z_{BA} or the self impedance Z_{AA} lies in the evaluation of g_o and g_s . g_o is $\exp(-jkR_1)/R_1$, and the computation is straightforward. The different techniques discussed in Section 2.2 are utilized to compute g_s either in the form $(g_1 - g_{sV})$ or $(-g_1 + G_{sV})$. In the reflection coefficient method g_{sV} is evaluated as outlined in Section 2.2b. In the "exact" solution g_{sV} is integrated numerically as explained in 2.2a for $\rho < 0.5\lambda$, and evaluated by a modified saddle point method of 2.2c for $\rho \geq 0.5\lambda$. For $\rho \geq (2|\epsilon|/k_1)\lambda$, the $(-g_1 + G_{sV})$ representation of g_s is used in the computation. User oriented computer programs [16-19] have been written along these lines

- [15] H. H. Chao and B. J. Strait, "Computer Programs for Radiation and Scattering by Arbitrary Configurations of Bent Wires," Scientific Report No. 7 on Contract No. F19628-68-C-0180, AFCRL-70-0374; Syracuse University, Syracuse, New York, September 1970.
- [16] B. J. Strait, T. K. Sarkar and D. C. Kuo, "Programs for Analysis of Radiation by Linear Arrays of Vertical Wire Antennas Over Imperfect Ground," Technical Report TR-74-1 on Contract No. F19628-73-C-0047, AFCRL-TR-74-0042; Syracuse University, Syracuse, NY: January 1974.
- [17] T. K. Sarkar and B. J. Strait, "Analysis of Radiation by Wire Antennas Over Imperfect Ground," Scientific Rept. No. 6 on Contract F19628-73-C-0047, AFCRL-TR-75-0337; Syracuse University, Syracuse, NY: May 1975.
- [18] T. K. Sarkar, "Analysis of Radiation by Arrays of Vertical Wire Antennas Over Imperfect Ground (Reflection-Coefficient Method)," IEEE Trans. Ant. and Propagat. vol. AP-23, September 1975, p. 749.
- [19] T. K. Sarkar, "Analysis of Radiation by Arrays of Parallel Vertical Wire Antennas Over Plane Imperfect Ground (Sommerfeld Formulation)," IEEE Trans. Ant. and Propagat., (to be published).

of thought.

Since the Reflection Coefficient Method utilizes a large argument approximation of the Hankel function, maximum error in this technique occurs in computing the near fields, or in other words the self impedance Z_{AA} . There is also another problem associated with the reflection coefficient method. When the specular angle θ as shown in Fig. 1 approaches 90° , the saddle point θ approaches the pole P_2 of Fig. 5. Hence the reflection coefficient method yields a good solution when two subsections A and B of Fig. 6 are away from the ground plane and separated by an appreciable distance yet which is not large. It has been found that the reflection coefficient method yields a result in the computation of impedance elements within 10% of the "exact solution" both in the real and imaginary parts as long as none of the elements are situated below a height of $(0.7/\sqrt{|\epsilon|})\lambda$ from the ground plane as shown in Fig. 6. This also ensures that when two elements are as much as 1000λ apart the accuracy of both real and imaginary parts of the impedance elements computed by this technique are still within 10% of the "exact" solution. It has also been observed that the restriction that no vertical elements can lie below a height of $(0.7/\sqrt{|\epsilon|})\lambda$ also ensures an accuracy of 10% in the impedance elements even for low values of dielectric constant ($|\epsilon| \approx 2$) of the ground plane. This indicates that so long as this restriction on the heights of the dipoles is maintained the contribution from the branch cut of B_3 is not too important.

2.4. Conclusion

Application of interpolatory quadrature formulas and a modified method of steepest descent to the infinite integrals encountered in

the Sommerfeld formulation have significantly reduced the time of computation necessary for treating the imperfect ground problem without significant loss of accuracy for evaluating these integrals. When a method of steepest descent is applied to the integrals of the exact Sommerfeld formulation, the reflection coefficient method falls out as the leading term in the series under certain conditions. The reflection coefficient method yields a result accurate to within 10% of the exact Sommerfeld formulation in both the real and imaginary parts of the impedance elements under all conditions of the ground so long as they are $(0.7/\sqrt{|\epsilon|})\lambda$ away from the surface. The reflection coefficient method does provide a good engineering result at about 15% of the computation time taken by the exact Sommerfeld formulation.

3. HORIZONTAL DIPOLES OVER A PLANE IMPERFECT GROUND

In this section, analysis of radiation is performed for parallel horizontal dipoles situated over a plane imperfect ground. As before, for near fields the semi-infinite integrals obtained in the Sommerfeld formulation are evaluated numerically using orthogonal interpolatory polynomials. For fields, away from the source a modified saddle-point method is applied to evaluate the same integrals to reduce the time of computation without any significant loss of accuracy. The reflection-coefficient method is also derived as a special case in the Sommerfeld formulation. The accuracy of the reflection-coefficient method is compared with that of the exact Sommerfeld formulation.

3.1. Sommerfeld Formulation

An elementary horizontal electric dipole of moment $I dx$ and oriented in the x -direction is located at a height z' above the horizontal imperfect ground plane, as shown in Fig. 7. In this case two components of the Hertzian vector, π_x and π_z of the electric type are necessary to specify the fields completely. Assuming a time variation $\exp(j\omega t)$ the Hertz potentials satisfy the following wave equations [6]

$$(\nabla^2 + k_1^2)\pi_1 = - \frac{I dx}{j\omega\epsilon_0\epsilon_1} \delta(x-x') \delta(y-y') \delta(z-z') \quad (3.1)$$

and

$$(\nabla^2 + k_2^2)\pi_2 = 0 \quad (3.2)$$

The electric and the magnetic field vectors are given by (2.5) and (2.6) respectively.

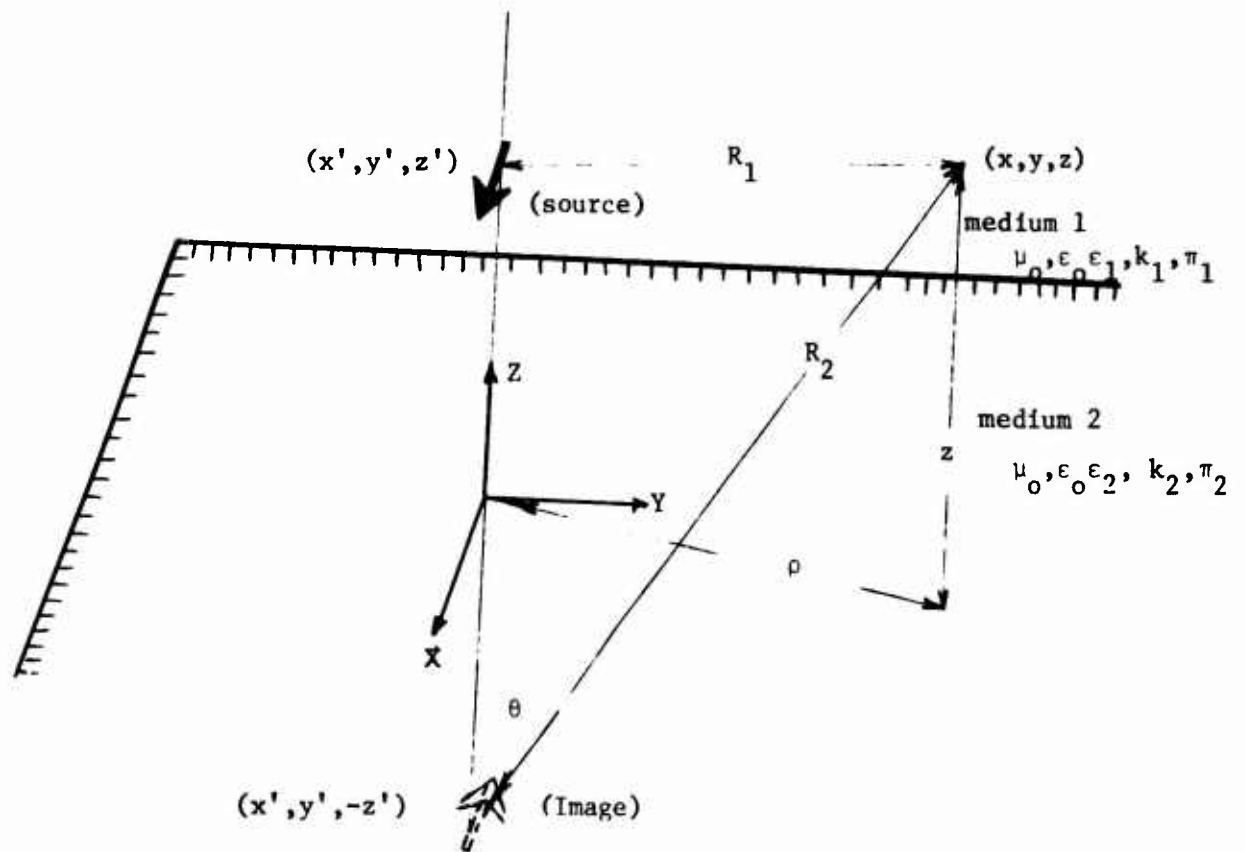


Fig. 7. A horizontal dipole over an imperfect ground plane.

From the continuity of E_y at the interface $z = 0$ it follows that

$$\frac{\partial \pi_{1x}}{\partial x} + \frac{\partial \pi_{1z}}{\partial z} = \frac{\partial \pi_{2x}}{\partial x} + \frac{\partial \pi_{2z}}{\partial z} \quad (3.3)$$

Similarly from the continuity of E_x and (3.3) it follows that

$$k_1^2 \pi_{1x} = k_2^2 \pi_{2x} \quad (3.4)$$

From the continuity of the magnetic field component H_x at the interface $z = 0$,

$$\epsilon_1 \frac{\partial \pi_{1z}}{\partial y} = \epsilon_2 \frac{\partial \pi_{2z}}{\partial y} \quad (3.5)$$

and from the continuity of H_y it follows that

$$\epsilon_1 \left(\frac{\partial \pi_{1x}}{\partial z} - \frac{\partial \pi_{1z}}{\partial x} \right) = \epsilon_2 \left(\frac{\partial \pi_{2x}}{\partial z} - \frac{\partial \pi_{2z}}{\partial x} \right) \quad (3.6)$$

Since (3.5) holds for all values of y ,

$$\epsilon_1 \pi_{1z} = \epsilon_2 \pi_{2z} \quad (3.7)$$

and because of (3.7), (3.6) reduces to

$$\epsilon_1 \frac{\partial \pi_{1x}}{\partial z} = \epsilon_2 \frac{\partial \pi_{2x}}{\partial z} \quad (3.8)$$

After the components π_{ix} have been solved for by using the wave equations (3.1) and (3.2) and the boundary conditions (3.4) and (3.8), the components π_{iz} can be obtained from (3.3) and (3.7). The complete solution for the Hertzian vectors has been given by Sommerfeld [6], Wait [20] Miller et. al. [3] and others, and can be written as follows:

- [20] J. R. Wait, "The Electromagnetic Fields of a Horizontal Dipole in the Presence of a Conducting Half-Space," Canadian J. of Phys., vol. 39, pp. 1017-1028, 1961.

$$^* H_{\pi_{1x}} = P' [\exp(-jk_1 R_1) / R_1$$

$$+ \int_0^\infty \frac{J_0(\lambda \rho)}{\sqrt{\lambda^2 - k_1^2}} \exp[-\sqrt{\lambda^2 - k_1^2} (z+z')] \frac{\sqrt{\lambda^2 - k_1^2} - \sqrt{\lambda^2 - k_2^2}}{\sqrt{\lambda^2 - k_1^2} + \sqrt{\lambda^2 - k_2^2}} \lambda d\lambda] \quad (3.9)$$

$$H_{\pi_{2x}} = 2P' \frac{\epsilon_1}{\epsilon_2} \int_0^\infty \frac{J_0(\lambda \rho) \exp[\sqrt{\lambda^2 - k_2^2} z - \sqrt{\lambda^2 - k_1^2} z']}{\sqrt{\lambda^2 - k_1^2} + \sqrt{\lambda^2 - k_2^2}} \lambda d\lambda \quad (3.10)$$

$$H_{\pi_{1z}} = 2P' \frac{\partial}{\partial x} \int_0^\infty J_0(\lambda \rho) \exp[-\sqrt{\lambda^2 - k_1^2} (z+z')] \frac{\sqrt{\lambda^2 - k_1^2} - \sqrt{\lambda^2 - k_2^2}}{k_2^2 \sqrt{\lambda^2 - k_1^2} + k_1^2 \sqrt{\lambda^2 - k_2^2}} \lambda d\lambda$$

$$\triangleq P' \frac{\partial}{\partial x} (g_2) \quad (3.11)$$

$$H_{\pi_{2z}} = 2P' \frac{\epsilon_1}{\epsilon_2} \frac{\partial}{\partial x} \int_0^\infty \frac{\sqrt{\lambda^2 - k_1^2} - \sqrt{\lambda^2 - k_2^2}}{k_2^2 \sqrt{\lambda^2 - k_1^2} + k_1^2 \sqrt{\lambda^2 - k_2^2}} J_0(\lambda \rho) \exp[\sqrt{\lambda^2 - k_2^2} z - \sqrt{\lambda^2 - k_1^2} z'] \lambda d\lambda \quad (3.12)$$

for $\text{Re}[\sqrt{\lambda^2 - k_{1,2}^2}] > 0$. Here ρ and R_1 are given by (2.16) and (2.17), and

$$P' = \frac{I \Delta x}{j \omega 4 \pi \epsilon_0 \epsilon_1} \quad (3.13)$$

Like $V_{\pi_{1z}}$ in (2.18), $H_{\pi_{1x}}$ can similarly be split into two parts

$$H_{\pi_{1x}} = H_{\pi_{1x}}^{\text{direct}} + H_{\pi_{1x}}^{\text{refl}}$$

where

$$H_{\pi_{1x}}^{\text{direct}} = P' \cdot \exp(-jk_1 R_1) / R_1 = P' \cdot g_0 \quad (3.14)$$

$$H_{\pi_{1x}}^{\text{refl}} = P' [-\exp(-jk_1 R_2) / R_2 + 2 \int_0^\infty \frac{J_0(\lambda \rho) \exp[-\sqrt{\lambda^2 - k_1^2} (z+z')]}{\sqrt{\lambda^2 - k_1^2} + \sqrt{\lambda^2 - k_2^2}} \lambda d\lambda]$$

$$\triangleq P' [-g_1 + g_{SH}] \quad (3.15)$$

* The superscript H represents the Hertz potentials due to a horizontal dipole, whereas V represents the potentials due to a vertical dipole.

and R_2 is given by (2.22). Here $H_{\pi_{1x}}^{\text{direct}}$ represents the particular solution of the wave equation (3.1) or the direct spherical wave contribution from the dipole source and $H_{\pi_{1x}}^{\text{refl}}$ can be interpreted as the complementary solution or a reflection term (reflection from the medium). It represents a superposition of plane waves, resulting from the reflection of the plane waves into which the original spherical wave from the horizontal dipole source was expanded. Upon reflection, the amplitude of each plane wave must be multiplied by a reflection coefficient $V(\lambda)$ quite different from $R(\lambda)$ as in the previous section because of a different orientation. The complex reflection coefficient $V(\lambda)$ takes into account the phase change as the wave travels from the source (x', y', z') to the boundary and then to the point of observation (x, y, z) . The reflection coefficient $V(\lambda)$ is then

defined as
$$\frac{\sqrt{\lambda^2 - k_1^2} - \sqrt{\lambda^2 - k_2^2}}{\sqrt{\lambda^2 - k_1^2} + \sqrt{\lambda^2 - k_2^2}}.$$
 As before, $H_{\pi_{2x}}$ can be interpreted as a partial transmission of the wave from medium 1 into medium 2. Unlike the elementary vertical dipole, the horizontal dipole over an imperfect ground plane needs two Hertz potentials to completely specify the fields.

The primary excitation $H_{\pi_{1x}}$ in this case gives rise to a secondary excitation $H_{\pi_{1z}}$ whose contribution is highly dependent on the complex dielectric constant of the ground (ϵ). This is because as $\epsilon \rightarrow \infty$, $H_{\pi_{1z}} \rightarrow 0$. Also, as $\epsilon \rightarrow 1$, $H_{\pi_{1z}} \rightarrow 0$. To get a physical interpretation of the nature of the fields due to $H_{\pi_{1z}}$, it is useful to consider the following form

$$H_{\pi_{1z}} = 2P' \int_0^\infty J_0'(\lambda \rho) \cos \phi \exp[-j\sqrt{k_1^2 - \lambda^2} (z+z')] \frac{\sqrt{\lambda^2 - k_1^2} - \sqrt{\lambda^2 - k_2^2}}{k_2 \sqrt{\lambda^2 - k_1^2} + k_1 \sqrt{\lambda^2 - k_2^2}} \lambda^2 d\lambda \quad (3.16)$$

where $\phi = \angle (x, \rho)$.

A principal distinction of the horizontal dipole as compared to the vertical dipole is its characteristic radiation implied by the factor $\cos \phi$. So

$$\begin{aligned}
 \kappa_{1z}^{2H} \pi_{1z} &= P' \int_0^\infty \left[-\left(1 - \frac{1}{\epsilon}\right) + \left(1 + \frac{1}{\epsilon}\right) \cdot \frac{\epsilon \sqrt{\lambda^2 - k_1^2} - \sqrt{\lambda^2 - k_2^2}}{\epsilon \sqrt{\lambda^2 - k_1^2} + \sqrt{\lambda^2 - k_2^2}} \right] J_0'(\lambda \rho) \cos \phi \times \\
 &\quad \exp[-j \sqrt{k_1^2 - \lambda^2} (z+z')] \cdot \lambda^2 d\lambda \\
 &= P' \left(1 - \frac{1}{\epsilon}\right) \frac{\partial^2}{\partial x \partial z} \left[\frac{\exp(-jk_1 R_2)}{R_2} \right] - P' \left(1 + \frac{1}{\epsilon}\right) \times \\
 &\quad \frac{\partial^2}{\partial x \partial z} \int_0^\infty \frac{\epsilon \sqrt{\lambda^2 - k_1^2} - \sqrt{\lambda^2 - k_2^2}}{\epsilon \sqrt{\lambda^2 - k_1^2} + \sqrt{\lambda^2 - k_2^2}} \frac{J_0(\lambda \rho) \exp[-j \sqrt{k_1^2 - \lambda^2} (z+z')]}{\sqrt{\lambda^2 - k_1^2}} \lambda d\lambda \quad (3.17)
 \end{aligned}$$

where $\epsilon = \epsilon_2/\epsilon_1$

The first term in the above expression can be interpreted as fields originating from a vertical octupole of strength $(1 - \frac{1}{\epsilon})$ situated at the image of the original horizontal dipole. The second term consists of infinite plane waves reflected from the ground plane and each multiplied by a different reflection coefficient $R(\lambda)$. It represents a superposition of plane waves resulting from the reflection of plane waves into which a spherical wave from a vertical octupolar source of strength $(1 + \frac{1}{\epsilon})$ was expanded. This representation is in no way unique. Interestingly, for large values of ϵ and when the horizontal dipole source is close to the ground the octupolar source which gives rise to $H_{\pi_{1z}}$ reduces to a quadrupolar source as illustrated.

$$H_{\pi 1z} \xrightarrow{z' \rightarrow 0} P' \frac{-2j}{k_1 \sqrt{\epsilon}} \frac{\partial}{\partial x} \left[\frac{\exp(-jk_1 R)}{R} \right] \quad (3.18)$$

$$H_{\pi 1x} \xrightarrow{z' \rightarrow 0} P' \frac{2j}{k_1 \sqrt{\epsilon}} \frac{\partial}{\partial z} \left[\frac{\exp(-jk_1 R)}{R} \right] \quad (3.19)$$

where

$$R = \left[(x - x')^2 + (y - y')^2 + z^2 \right]^{1/2} \quad (3.20)$$

Thus, for the source close to the ground plane and for large ϵ , the horizontal dipole appears as a quadrupole. Also, $H_{\pi 2z}$ can be interpreted as representing the waves induced in medium 2 by the secondary excitations generated in medium 1 and represented as $H_{\pi 1z}$.

3.2. Evaluation of Mutual Impedance Between Two Parallel Horizontal Dipoles

In this section an expression is obtained for the mutual impedance between two x-directed current elements of lengths ℓ_A and ℓ_B carrying current distributions I_A and I_B , respectively, and situated over a horizontal ground plane. The corresponding configuration is presented in Fig. 8. The electric field \vec{E}_A in medium 1 due to the current element I_A is given by

$$\begin{aligned} \vec{E}_A &= [k_1^2 + \vec{\nabla} \cdot \vec{\nabla}] [\vec{\pi}_1] \\ &= k_1^2 (\vec{\pi}_{1x} + \vec{\pi}_{1z}) + \left(\frac{\partial \pi_{1x}}{\partial x} + \frac{\partial \pi_{1z}}{\partial z} \right) \end{aligned} \quad (3.21)$$

For an elemental dipole of moment $I \Delta x$, the expression $\left(\frac{\partial \pi_{1x}}{\partial x} + \frac{\partial \pi_{1z}}{\partial z} \right)$ can be written in a simpler form. By using (3.11), (3.14) and (3.15),

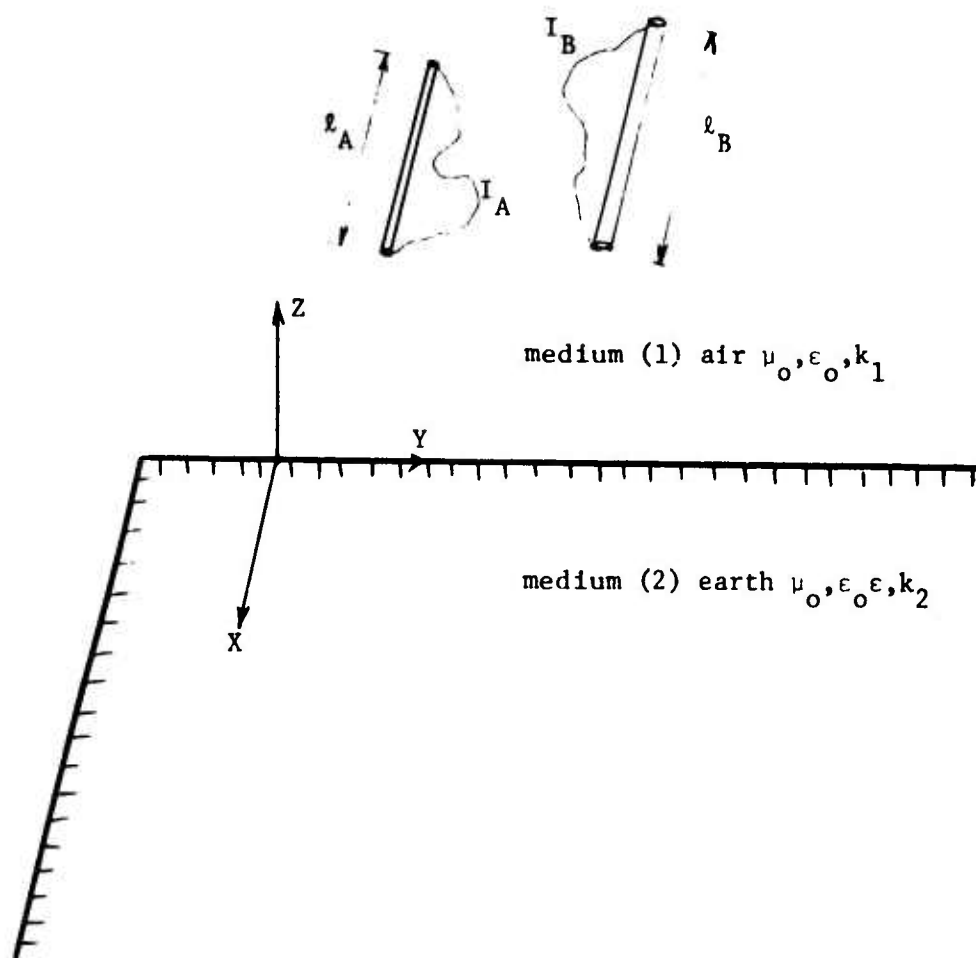


Fig. 8. Two parallel x -directed horizontal dipoles of lengths ℓ_A and ℓ_B having a current distribution of I_A and I_B situated over a plane earth.

$$\begin{aligned}
\frac{\partial \pi}{\partial x} \frac{1x}{\partial x} + \frac{\partial \pi}{\partial z} \frac{1z}{\partial z} &= P' \cdot \frac{\partial}{\partial x} [g_0 - g_1 + (g_{sH} + \frac{\partial}{\partial z} \{g_2\})] \\
&= P' \cdot \frac{\partial}{\partial x} [g_0 - g_1 + 2k_1^2 \int_0^\infty \frac{J_0(\lambda \rho) \exp[-\sqrt{\lambda^2 - k_1^2} (z + z')] }{k_2^2 \sqrt{\lambda^2 - k_1^2} + k_1^2 \sqrt{\lambda^2 - k_2^2}} \lambda d\lambda] \\
&= P' \cdot \frac{\partial}{\partial x} [g_0 - g_1 + G_{sV}/\epsilon] \quad \text{(from 2.24)}
\end{aligned}$$

$$\underline{A} \quad P' \cdot \frac{\partial}{\partial x} [g_0 - g_1 + g_3] \quad (3.22)$$

Hence the x-directed field for a current distribution I_A is given by
(3.21)

$$\begin{aligned}
E_A^x &= - \frac{j\omega\mu_0}{4\pi} \int_{\ell_A} I_A (g_0 - g_1 + g_{sH}) dx'_A \\
&\quad + \frac{\partial}{\partial x} \left[\frac{1}{j4\pi\omega\epsilon_0} \int_{\ell_A} I_A \frac{\partial}{\partial x} \{(g_0 - g_1 + g_3)\} dx'_A \right] \quad (3.23)
\end{aligned}$$

since $\frac{\partial g_0}{\partial x} = - \frac{\partial g_0}{\partial x'_A}$, $\frac{\partial g_1}{\partial x} = - \frac{\partial g_1}{\partial x'_A}$ and $\frac{\partial g_3}{\partial x} = - \frac{\partial g_3}{\partial x'_A}$

and assuming the current I_A goes to zero at the ends of the open wires,
the derivative $\frac{\partial}{\partial x}$ can be transferred to $\frac{\partial}{\partial x'_A}$ operating on I_A so that

$$\begin{aligned}
E_A^x &= - \frac{j\omega\mu_0}{4\pi} \int_{\ell_A} I_A (g_0 - g_1 + g_{sH}) dx'_A \\
&\quad + \frac{\partial}{\partial x} \left[\frac{1}{j4\pi\omega\epsilon_0} \int_{\ell_A} \frac{\partial I_A}{\partial x'_A} (g_0 - g_1 + g_3) dx'_A \right] \quad (3.24)
\end{aligned}$$

The mutual impedance Z_{BA} between the current element I_A and another
current element I_B oriented in the same direction (*) is

$$\begin{aligned}
Z_{BA} &= - \int_{\ell_B} E_A^x I_B dx'_B \\
&= \frac{j\omega\mu_0}{4\pi} \int_{\ell_B} I_B dx'_B \int_{\ell_A} I_A (g_0 - g_1 + g_{SH}) dx'_A \\
&\quad - \frac{1}{j4\pi\omega\epsilon_0} \int_{\ell_B} I_B dx'_B \frac{\partial}{\partial x} \left[\int_{\ell_A} \frac{dI_A}{dx'_A} (g_0 - g_1 + g_3) dx'_A \right] \quad (3.25)
\end{aligned}$$

By transferring the derivative to I_B and assuming I_B goes to zero at the end of the wires,

$$\begin{aligned}
Z_{BA} &= \frac{j\omega\mu_0}{4\pi} \int_{\ell_B} I_B dx'_B \int_{\ell_A} I_A (g_0 - g_1 + g_{SH}) dx'_A \\
&\quad + \frac{1}{j4\pi\omega\epsilon_0} \int_{\ell_B} \frac{dI_B}{dx'_B} dx'_B \int_{\ell_A} \frac{dI_A}{dx'_A} (g_0 - g_1 + g_3) dx'_A \quad (3.26)
\end{aligned}$$

computation of mutual impedance between two parallel horizontal dipoles over an imperfect ground plane then amounts to evaluating the integrals of g_{SH} and g_3 . This is dealt with in the next section.

3.3. Numerical Evaluation of the Integrals

In this section the integrals of g_{SH} and g_3 are evaluated in an essentially exact manner. Where applicable the method of steepest descent has been applied to reduce the computation time without any significant reduction or loss in accuracy.

a) Exact Solution. The problem of determining the mutual impedance Z_{BA} amounts to evaluating the semi-infinite integrals g_{SH} and g_3 in

an essentially exact manner. Since the integrals are very similar to those of (2.23) and (2.24), the integration scheme as explained in section 2.2a, [3, 17] is used.

One of the major problems associated with this technique is that for large values of ρ there are large numerical errors, as explained in 2.2a. The other problem is that when the current elements are below a height of 0.03λ from the ground plane the integrals g_{sH} and g_3 in (3.11) and (3.15) become oscillatory and hence the quadrature formulas explained in Appendix A fail. Therefore it is not possible to analyze antennas situated at distances less than 0.03λ from the ground plane using this procedure.

b) Modified Method of Steepest Descent: For large ρ a modified method of steepest descent can be applied to the integral g_3 (because of a pole in the integrand) and a method of steepest descent can be applied to the integral g_{sH} to reduce the computation time without significant loss in accuracy. Making the following substitutions, as suggested by (2.26), (2.27), (2.36), (2.37) and (2.38), the integrals can be written as

$$g_{sH} = \int_{\Gamma_1} \left(\frac{2k_1 \sin \beta}{\pi R_2 \sin \theta} \right)^{1/2} \frac{\cos \beta}{\cos \beta + \sqrt{\epsilon - \sin^2 \beta}} \exp[j\{-\pi/4 - k_1 R_2 \cos(\beta - \theta)\}] d\beta \quad (3.27)$$

$$g_3 = \int_{\Gamma_1} \left(\frac{2k_1 \sin \beta}{\pi R_2 \sin \theta} \right)^{1/2} \frac{\cos \beta}{\epsilon \cos \beta + \sqrt{\epsilon - \sin^2 \beta}} \exp[j\{-\pi/4 - k_1 R_2 \cos(\beta - \theta)\}] d\beta \quad (3.28)$$

where Γ_1 is a path in the complex β -plane as shown in Fig. 5. The large argument approximations for the Hankel functions have been justified [9]. The above

integrals are then evaluated by using (B.4) for g_{sH} (since the expression of g_{sH} does not have any pole near the saddle point $\beta = \theta$) for g_3 , respectively. Hence,

$$g_{sH} = \frac{2 \cos \theta}{\cos \theta + \sqrt{\epsilon - \sin^2 \theta}} \frac{\exp(-jk_1 R_2)}{R_2} \quad (3.29)$$

[taking only the spherical-wave part or the first term of the saddle-point method] and

$$g_3 = \left(\frac{4\pi k_1 j}{R_2}\right)^{1/2} \frac{\cos \theta}{\cos \theta - \sqrt{\frac{1}{\epsilon+1}}} \frac{\sqrt{\epsilon - \sin^2 \theta} - \epsilon \cos \theta}{\epsilon^2 - 1} \frac{\exp[-jk_1 R_2 - W^2] \operatorname{erfc}(jW)}{\left\{1 + \frac{\cos \theta}{\sqrt{\epsilon+1}} + \frac{\sqrt{\epsilon} \sin \theta}{\sqrt{\epsilon+1}}\right\}^{1/2}} \quad (3.30)$$

where W^2 is given by (2.55)

An user-oriented computer program has been written along these lines of analysis and is available [17,21].

3.4. Reflection - Coefficient Method

For field points far away from the source and away from the ground plane the method of steepest descent is applied to evaluate the integrals g_{sH} and g_3 . For both source and field points near the ground plane, the effect of a pole which may exist near the vicinity of a saddle point (in g_3) is neglected. Making the following transformations as suggested by (2.26), (2.27), (2.36), (2.37) and (2.38), $H_{\pi_{1x}}^{\text{refl}}$ and $H_{\pi_{1z}}^H$ can be expressed as

-
- [21] T. K. Sarkar, "Analysis of Radiation by Arrays of Parallel Horizontal Wire Antennas Over Plane Imperfect Ground (Sommerfeld Formulation)," IEEE Trans. Ant. and Propagat., (to be published).

$$H_{\pi_{1x}}^{\text{refl}} = \frac{P'}{2} \int_{\Gamma_1} \left(\frac{2k_1 \sin \beta}{\pi R_2 \sin \theta} \right)^{1/2} \exp[j\{-\pi/4 - k_1 R_2 \cos(\beta - \theta)\}] \times \frac{\cos \beta - \sqrt{\epsilon - \sin^2 \beta}}{\cos \beta + \sqrt{\epsilon - \sin^2 \beta}} d\beta \quad (3.31)$$

$$H_{\pi_{1z}} = P' \cos \phi \int_{\Gamma_1} \exp[j\{-\pi/4 - k_1 R_2 \cos(\beta - \theta)\}] \left(\frac{2k_1 \sin \beta}{\pi R_2 \sin \theta} \right)^{1/2} \frac{\cos \beta - \sqrt{\epsilon - \sin^2 \beta}}{\epsilon \cos \beta + \sqrt{\epsilon - \sin^2 \beta}} \sin \beta \times \cos \beta d\beta \quad (3.32)$$

since

$$H_1^{(2)}(\lambda \rho) \xrightarrow{|\lambda \rho| \rightarrow \infty} \left(\frac{2}{\pi \lambda \rho} \right)^{1/2} \exp[-j(\lambda \rho - 3\pi/4)] \quad (3.33)$$

The contour of integration Γ_1 is defined in Fig. 5. Application of the saddle-point method as given by (B.4) to (3.31) and (3.32) yields

$$H_{\pi_{1x}}^{\text{refl}} = P' \frac{\cos \theta - \sqrt{\epsilon - \sin^2 \theta}}{\cos \theta + \sqrt{\epsilon - \sin^2 \theta}} \frac{\exp(-jk_1 R_2)}{R_2} \quad (3.34)$$

$$H_{\pi_{1z}} = 2P' \cos \phi \sin \theta \cos \theta \frac{\cos \theta - \sqrt{\epsilon - \sin^2 \theta}}{\epsilon \cos \theta + \sqrt{\epsilon - \sin^2 \theta}} \frac{\exp(-jk_1 R_2)}{R_2} \quad (3.35)$$

The expressions for the far field due to the reflected rays only, are given by [14],

$$E_{\rho}^{\text{refl}} = -j\omega\mu_0 \cos \theta [H_{\pi_{1x}}^{\text{refl}} \cos \theta \cos \phi - H_{\pi_{1z}}^{\text{refl}} \sin \theta] \quad (3.36)$$

$$E_z^{\text{refl}} = j\omega\mu_0 \sin \theta [H_{\pi_{1x}}^{\text{refl}} \cos \theta \cos \phi - H_{\pi_{1z}}^{\text{refl}} \sin \theta] \quad (3.37)$$

$$E_{\phi}^{\text{refl}} = j\omega\mu_0 \sin \phi H_{\pi_{1x}}^{\text{refl}} \quad (3.38)$$

this defined plane) by the specular plane wave TM reflection coefficient and E_ϕ (- field perpendicular to this defined plane) by the negative of the specular plane-wave TE reflection coefficient. The fields E_ρ , E_ϕ and E_z used for this case are assumed not to originate from the source dipole, but from the image of the source dipole.

The mutual impedance between two parallel horizontal electric dipoles over an imperfect ground plane can be computed as indicated. An user-oriented computer program is available using the reflection-coefficient method for treating problems of this type [22,23].

3.5. Comparison of Accuracy Between the Reflection Coefficient Method and the Exact Sommerfeld Formulation

In the case of the horizontal dipoles only $H_{\pi_{1z}}$ has a singularity and not $H_{\pi_{1x}}$. But $H_{\pi_{1z}}$ in (3.16) has a $\cos \phi$ variation which indicates that the effect of the singularity would be maximum when the field due to the dipole is computed in a plane containing the dipole and perpendicular to the ground plane. When the field is computed along a plane perpendicular to the axis of the dipole, the effect of the singularity is zero. Also, from (3.22), the contribution from the singularity is less for the corresponding vertical dipole by a factor of $1/\epsilon$. Hence

-
- [22] T. K. Sarkar and B. J. Strait, "Analysis of Radiation by Arrays of Parallel Horizontal Wire Antennas Over Imperfect Ground," Scientific Report No. 5 on Contract F19628-73-C-0047, AFCRL-TR-74-0538, Syracuse University, Syracuse, New York: September 1974.
 - [23] T. K. Sarkar, "Analysis of Radiation by Arrays of Horizontal Wire Antennas Over Imperfect Ground," (Reflection Coefficient Method)," IEEE Trans. Ant. and Propagat., (to be published).

Let the specular TE and TM reflection coefficients be denoted by Γ_{TE} and Γ_{TM} , respectively, and defined by

$$\Gamma_{TE} = \frac{\cos \theta - \sqrt{\epsilon - \sin^2 \theta}}{\cos \theta + \sqrt{\epsilon - \sin^2 \theta}} \quad (3.39)$$

and Γ_{TM} by (2.48).

Since,

$$H_{\pi_{1x}}^{\text{refl}} \cos \theta \cos \phi - H_{\pi_{1z}} \sin \theta = -P' \cos \theta \cos \phi \Gamma_{TM} \exp(-jk_1 R_2)/R_2$$

the far field expressions in (3.36) - (3.38) reduce to

$$\begin{aligned} E_{\rho}^{\text{refl}} &= j\omega\mu_0 \cos^2 \theta \cos^2 \phi \Gamma_{TM} P' \exp(-jk_1 R_2)/R_2 \\ &= \Gamma_{TM} \cdot (\text{far } E_{\rho} \text{ field from the image due to a} \\ &\quad \text{perfectly conducting ground plane}) \end{aligned} \quad (3.40)$$

$$\begin{aligned} E_z^{\text{refl}} &= -j\omega\mu_0 \sin \theta \cos \theta \cos \phi \Gamma_{TM} P' \exp(-jk_1 R_2)/R_2 \\ &= \Gamma_{TM} \cdot (\text{far } E_z \text{ field from the image due to a} \\ &\quad \text{perfectly conducting ground plane}) \end{aligned} \quad (3.41)$$

$$\begin{aligned} E_{\phi}^{\text{refl}} &= j\omega\mu_0 \sin \phi \Gamma_{TE} P' \exp(-jk_1 R_2)/R_2 \\ &= -\Gamma_{TE} \cdot (\text{far } E_{\phi} \text{ field from the image due to a} \\ &\quad \text{perfectly conducting ground plane}). \end{aligned} \quad (3.42)$$

A physical interpretation can be given for these formulas. A plane of incidence can be defined as a plane passing through the mid-point of the horizontal dipole and the field point in question and that is also perpendicular to the ground plane. Then the contributions from the reflected ray can be obtained by multiplying E_{ρ} and E_z (- fields in

it is expected that the reflection-coefficient method would give a better approximation to the exact Sommerfeld formulation than for the vertical dipole case. Also, as before, for the reflection-coefficient method the maximum error occurs in the computation of the near fields and hence, the self impedances. It has been found that for the worst case of two coplanar horizontal dipoles (for $\phi = 0$) the reflection-coefficient method yields a result within 10% of the exact Sommerfeld formulation both in the real and imaginary parts of impedance elements, as long as the dipoles are away by at least $(0.25/\sqrt{\epsilon})\lambda$ from the ground plane. For the reflection coefficient method, there is still another restriction on the distances between two horizontal dipoles. This is because as the distance gets larger the saddle point θ approaches the pole at $\pi/2$ [in g_3 (3.22)]. It has been observed that the horizontal dipoles should lie within a cone whose semi-vertical angle is 70° in order that the reflection-coefficient method yield results within 10% of the exact Sommerfeld formulation both in the real and imaginary parts of the impedance elements. The apex of the cone is the image of the middle point of the source dipole. This is illustrated in Fig. 9. This implies that the maximum lengths of the horizontal dipoles for which 10% accuracy can be obtained in the evaluation of the impedance elements by the reflection-coefficient method is

$$L_{\text{critical}} = 2h \tan 70^\circ \approx 5.5h \quad (3.43)$$

as indicated in Fig. 9.

Also for large ϵ and large distances away from the source ${}^H\pi_{1x}$ and ${}^H\pi_{1z}$ in (3.18) and (3.19) can be rewritten as

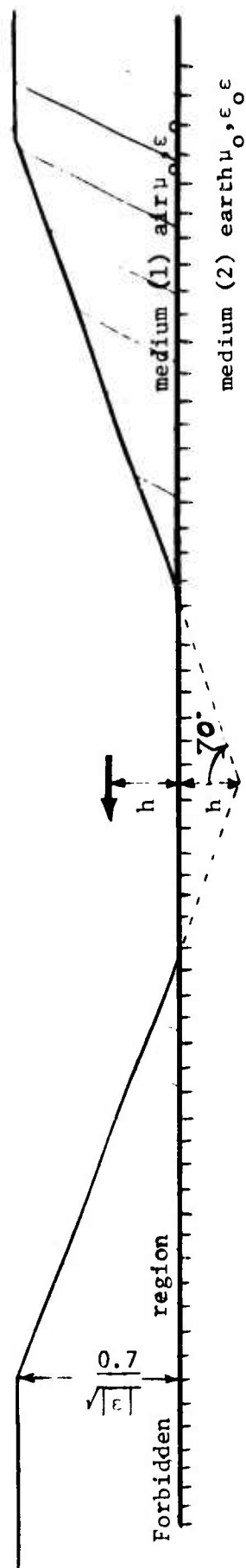


Fig. 9. Range of validity of the reflection coefficient method.

$$H_{\pi_{1x}} = P' \frac{2j}{k_1 \sqrt{\epsilon}} \frac{z}{R} \frac{\partial}{\partial R} \frac{\exp(-jk_1 R)}{R} \quad (3.44)$$

$$H_{\pi_{1z}} = P' \frac{-2j}{k_1 \sqrt{\epsilon}} \frac{\rho}{R} \frac{\partial}{\partial R} \frac{\exp(-jk_1 R)}{R} \quad (3.45)$$

Hence from (3.44) and (3.45) $H_{\pi_{1x}}$ and $H_{\pi_{1z}}$ have the ratio z/ρ which is very small at great distances from the transmitter. The field of transmission of a horizontal antenna has the same character as the field of transmission of a vertical antenna except for the ϕ dependence. It is then expected that the restriction on the length of a horizontal antenna can be removed if it is situated at least $(0.7/\sqrt{\epsilon})\lambda$ away from the ground plane (as from 2.3). For the worst case, $\phi = 0$, it has been found that the reflection-coefficient method yields a solution within 10% of the exact Sommerfeld formulation both in the real and imaginary parts of impedance elements even when two horizontal currents are as much as 1000λ apart.

3.6. Conclusion

Application of interpolatory quadrature formulas and a modified method of steepest descent to the infinite integrals encountered in the Sommerfeld formulation have significantly reduced the time of computation without appreciable loss of accuracy for evaluating these integrals. When a method of steepest descent is applied to the integrals of the exact Sommerfeld formulation the reflection-coefficient method falls out as the leading term in the series under certain conditions. The reflection-coefficient

method yields a result within 10% of the exact Sommerfeld formulation in both the real and imaginary parts of the impedance elements provided the antennas are no longer than $5.5h$ where h , the height of the antennas above the ground plane, can be no less than $(0.25/\sqrt{\epsilon})\lambda$. For large ϵ , the restriction on the lengths of the antenna can be relaxed so long as they are situated at least $(0.7/\sqrt{\epsilon})\lambda$ away from the ground plane.

4. ARBITRARY ORIENTED WIRE ANTENNAS OVER IMPERFECT GROUND

In this section expressions for mutual impedance between two arbitrary oriented wire antennas over plane imperfect ground are derived both by the Sommerfeld formulation and by the reflection-coefficient method. The problem configuration consists of two arbitrarily oriented current elements having a current distribution I_A and I_B . They are situated over a plane imperfect ground as shown in Fig. 10. The ground is characterized by the complex dielectric constant ϵ . It is possible for I_A and I_B to overlap one another, thereby forming a wire junction. The method of analysis is the same as presented in the last two sections.

4.1. Exact Sommerfeld Formulation

In order to compute the mutual impedance between two arbitrarily oriented current elements, the source current element \vec{I}_A is split up into three components I_A^x , I_A^y and I_A^z . The total electric field \vec{E} is then the summation of $\vec{E}_{I_A^x}$, $\vec{E}_{I_A^y}$ and $\vec{E}_{I_A^z}$ - fields due to the component current elements I_A^x , I_A^y and I_A^z as in Fig. 10. Hence from (2.5), (3.11), (3.14) and (3.15) the electric field due to I_A^x can be written as

$$\begin{aligned} \vec{E}_{I_A^x} = \int_{\ell_A} & \left[-\frac{j\omega\mu}{4\pi} + \frac{\vec{\nabla} \vec{\nabla} \cdot}{j\omega 4\pi\epsilon_0} \right] [x I_A^x (g_0 - g_1 + g_{SH}) \\ & + 2 I_A^x \frac{\partial}{\partial x} (g_2)] d\ell_A \end{aligned} \quad (4.1)$$

Similarly for

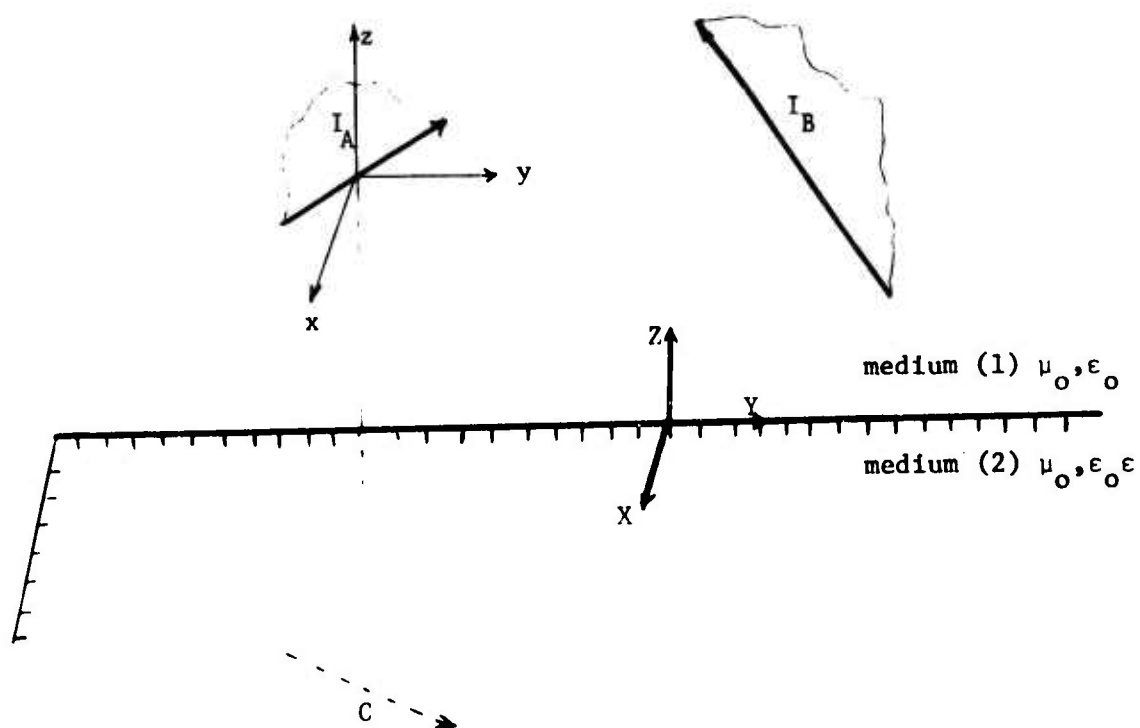


Fig. 10. Arbitrary oriented elements over an imperfect ground plane.

$$\vec{E}_{I_A^y} = \int_{\ell_A} \left[-\frac{j\omega\mu_0}{4\pi} + \frac{\vec{\nabla} \cdot \vec{\nabla}}{j\omega 4\pi\epsilon_0} \right] [\hat{y} I_A^y (g_0 - g_1 + g_{sH}) + 2 I_A^y \frac{\partial}{\partial y} (g_2)] d\ell_A \quad (4.2)$$

and from (2.5), (2.19) and (2.24) the field is

$$\vec{E}_{I_A^z} = \int_{\ell_A} \left[-\frac{j\omega\mu_0}{4\pi} + \frac{\vec{\nabla} \cdot \vec{\nabla}}{j\omega 4\pi\epsilon_0} \right] [2 I_A^z (g_0 - g_1 + G_{sV})] d\ell_A \quad (4.3)$$

Next some relations are presented which are very helpful in deriving a formula for mutual impedance between \vec{I}_A and \vec{I}_B . First

$$\frac{\partial}{\partial x} (g_{sH}) + \frac{\partial}{\partial z} \frac{\partial}{\partial x} (g_2) = \frac{\partial}{\partial x} \left(-\frac{G_{sV}}{\epsilon} \right) = -\frac{\partial}{\partial x_A'} \left(-\frac{G_{sV}}{\epsilon} \right) = -\frac{\partial}{\partial x_A'} (g_3)$$

is obtained from (3.22). Also,

$$\frac{\partial}{\partial y} (g_{sH}) + \frac{\partial}{\partial z} \frac{\partial}{\partial y} (g_2) = \frac{\partial}{\partial y} \left(-\frac{G_{sV}}{\epsilon} \right) = -\frac{\partial}{\partial y_A'} \left(-\frac{G_{sV}}{\epsilon} \right) = -\frac{\partial}{\partial y_A'} (g_3) ;$$

It is well-known that

$$\frac{\partial}{\partial p} (g_0) = -\frac{\partial}{\partial p_A'} (g_0) , \text{ where } p \text{ may be 'x', 'y' or 'z' ,}$$

$$\frac{\partial}{\partial q} (g_1) = -\frac{\partial}{\partial q_A'} (g_1) , \text{ where } q \text{ may be 'x' or 'y' ,}$$

$$\frac{\partial}{\partial q} (g_{sH}) = -\frac{\partial}{\partial q_A'} (g_{sH}) ; \frac{\partial}{\partial q} (g_2) = -\frac{\partial}{\partial q_A'} (g_2) ;$$

$$\frac{\partial}{\partial z} (g_1) = \frac{\partial}{\partial z_A'} (g_1) \text{ and } \frac{\partial}{\partial z} (G_{sV}) = \frac{\partial}{\partial z_A'} (G_{sV}) .$$

Applying the above identities the total E-field can be obtained in the following form after some algebraic manipulations on (4.1), (4.2) and (4.3).

$$\begin{aligned}
\vec{E}_A &= \vec{E}_{I_A^x} + \vec{E}_{I_A^y} + \vec{E}_{I_A^z} \\
&= -\frac{j\omega\mu_0}{4\pi} \int_{\ell_A} [\vec{I}_A (g_0 - g_1 + g_{sH}) + 2 \{-I_A^z Q - \vec{I}_A \cdot \nabla'_A (g_2)\}] d\ell_A \\
&\quad + \frac{\vec{\nabla}}{j\omega 4\pi\epsilon_0} \int_{\ell_A} [-\vec{I}_A \cdot \vec{\nabla}'_A (g_0 - g_1 + g_3) - I_A^z T] d\ell_A
\end{aligned} \tag{4.4}$$

where Q and T are given by the following:

$$\begin{aligned}
Q &= -[G_{sV} + \frac{\partial}{\partial z'_A} (g_2) - g_{sH}] \\
&= 2 \int_0^\infty J_0(\lambda\rho) \exp[-\sqrt{\lambda^2 - k_1^2} (z + z')] \frac{\{\sqrt{\lambda^2 - k_1^2} - \sqrt{\lambda^2 - k_2^2}\}^2}{k_2^2 \sqrt{\lambda^2 - k_1^2} + k_1^2 \sqrt{\lambda^2 - k_2^2}} \lambda d\lambda
\end{aligned} \tag{4.5}$$

and

$$T = \frac{\partial}{\partial z'_A} [2g_1 - G_{sV} - g_3] = g_2 \cdot k_1^2 \tag{4.6}$$

Transferring the derivative ($\vec{\nabla}'_A$) operating on the Green's function over to the current (\vec{I}_A) and assuming the current to be zero at the ends of the open wires,

$$\begin{aligned}
\vec{E}_A &= -\frac{j\omega\mu_0}{4\pi} \int_{\ell_A} [\vec{I}_A (g_0 - g_1 + g_{sH}) + 2 \{-I_A^z Q + \frac{dI_A}{d\ell_A} g_2\}] d\ell_A \\
&\quad + \frac{\vec{\nabla}}{j\omega 4\pi\epsilon_0} \int_{\ell_A} [\frac{dI_A}{d\ell_A} (g_0 - g_1 + g_3) - I_A^z T] d\ell_A
\end{aligned} \tag{4.7}$$

The mutual impedance between the two current elements \vec{I}_A and \vec{I}_B can then be expressed as

$$Z_{AB} = - \int_{\ell_B} \vec{E}_A \cdot \vec{I}_B d\ell_B \tag{4.8}$$

After some algebraic manipulations, the mutual impedance reduces to

$$\begin{aligned}
 Z_{AB} = & \frac{j\omega\mu_0}{4\pi} \int_{\ell_B} d\ell_B \int_{\ell_A} d\ell_A [\vec{I}_A \cdot \vec{I}_B (g_0 - g_1 + g_{SH}) + I_B^z \{ \frac{dI_A}{d\ell_A} g_2 - I_A^z Q \}] \\
 & + \frac{1}{j\omega 4\pi\epsilon_0} \int_{\ell_B} \frac{dI_B}{d\ell_B} d\ell_B \int_{\ell_A} d\ell_A [\frac{dI_A}{d\ell_A} (g_0 - g_1 + g_3) - I_A^z g_2 k_1^2] \quad (4.9)
 \end{aligned}$$

For $\rho < 0.5\lambda$, the semi-infinite integrals in g_{SH} , g_2 , g_3 and Q are computed in an essentially exact manner along a contour shown in Fig. 2.

For $\rho \geq 0.5\lambda$, a modified method of steepest descent is applied to take into account the pole near the saddle point, and the integrals can be expressed as follows:

$$Q = -g_3 (\cos \theta - \sqrt{\epsilon - \sin^2 \theta})^2 \quad (4.10)$$

$$g_2 = jg_3 (\cos \theta - \sqrt{\epsilon - \sin^2 \theta})/k_1 \quad (4.11)$$

and g_{SH} and g_3 are given by (3.29) and (3.30).

A user-oriented computer program has been written and is presented in a later report. The underlying mathematics of the program is relatively straightforward once the general formula for Z_{AB} in (4.9) is available.

4.2. Reflection-Coefficient Method

In order to find the mutual impedance between two arbitrarily oriented current elements over the plane surface of an imperfectly conducting earth, the effects of the direct ray and reflected ray are considered separately. The effect of the direct ray is straightforward and is the same as in [15]. In order to obtain the effects of the reflected ray a local co-ordinate system centered at the middle point of dipole A

is chosen. The x and z axes of the co-ordinate system are oriented in such a way that the x-z plane passes through the center-point of dipole B. Also the x-y plane is parallel to the imperfectly conducting earth. The currents of element A are now split up into three components each being parallel to the local co-ordinate axes chosen. As seen from (2.49), (2.50), (3.40)-(3.42), the effect of the reflected ray is equivalent to taking the original current element and placing it at the image point C as in Fig. 10. Then the contribution to the reflected ray due to I_A^x is $-\Gamma_{TM} \frac{E_A^x}{I_A^x} + \Gamma_{TE} \frac{E_A^y}{I_A^x}$ where E_A^x , E_A^y and E_A^z are the three components of the electric field generated by I_A^x . Similarly for I_A^y the corresponding contribution is $-\Gamma_{TM} \frac{E_A^x}{I_A^y} + \Gamma_{TE} \frac{E_A^y}{I_A^y}$ and for I_A^z , $\Gamma_{TM} \frac{E_A^x}{I_A^z} + \Gamma_{TE} \frac{E_A^y}{I_A^z}$. Hence the total E-field due to the reflected ray is given by

$$\begin{aligned}
 \vec{E}^I &= \Gamma_{TM} (\hat{x} E_{I_A^z}^x + 2 E_{I_A^z}^z - \hat{x} E_{I_A^x}^x - 2 E_{I_A^x}^z - \hat{x} E_{I_A^y}^x - 2 E_{I_A^y}^z) \\
 &+ \hat{y} \Gamma_{TE} (E_{I_A^x}^y + E_{I_A^y}^y + E_{I_A^z}^y) \\
 &= -\frac{j\omega\mu_0}{4\pi} \int_{\ell_A} [-\Gamma_{TM} \vec{I}_A^x + \Gamma_{TE} \vec{I}_A^y + \Gamma_{TM} \vec{I}_A^z] \frac{e^{-jk_1 R_2}}{R_2} d\ell_A \\
 &- \frac{\Gamma_{TM}}{j\omega 4\pi\epsilon_0} \vec{\nabla} \int_{\ell_A} \frac{dI_A}{d\ell_A} \frac{e^{-jk_1 R_2}}{R_2} d\ell_A + \frac{\Gamma_{TM}}{j\omega 4\pi\epsilon_0} \hat{y} \int_{\ell_A} \frac{dI_A}{d\ell_A} \frac{\partial}{\partial y} \left(\frac{e^{-jk_1 R_2}}{R_2} \right) d\ell_A \\
 &+ \frac{\Gamma_{TE}}{j\omega 4\pi\epsilon_0} \hat{y} \int_{\ell_A} \left[\frac{I_A^y}{R_2} \frac{\partial}{\partial R_2} \left(\frac{e^{-jk_1 R_2}}{R_2} \right) + (\vec{I}_A \cdot \vec{R}_2) \frac{\partial}{\partial y} \left(\frac{1}{R_2} \frac{\partial}{\partial R_2} \left\{ \frac{e^{-jk_1 R_2}}{R_2} \right\} \right) \right] d\ell_A
 \end{aligned}
 \tag{4.12}$$

The mutual impedance between the two current elements I_A and I_B is defined as

$$\begin{aligned}
 Z^I &= - \int_{\ell_B} \vec{E}^I \cdot \vec{I}_B d\ell_B \\
 &= \frac{j\omega\mu_0}{4\pi} \int_{\ell_B} \int_{\ell_A} \{ -\Gamma_{TM} I_A^x I_B^x + \Gamma_{TE} I_A^y I_B^y + \Gamma_{TM} I_A^z I_B^z \} \frac{e^{-jk_1 R_2}}{R_2} d\ell_A d\ell_B \\
 &\quad - \frac{\Gamma_{TM}}{j\omega 4\pi \epsilon_0} \int_{\ell_B} \int_{\ell_A} \frac{dI_B}{d\ell_B} \frac{dI_A}{d\ell_A} \frac{e^{-jk_1 R_2}}{R_2} d\ell_A d\ell_B \\
 &\quad - \frac{\Gamma_{TM}}{j\omega 4\pi \epsilon_0} \int_{\ell_B} I_B^y d\ell_B \int_{\ell_A} \frac{dI_A}{d\ell_A} \frac{R_y}{R_2} \frac{\partial}{\partial R_2} \left(\frac{e^{-jk_1 R_2}}{R_2} \right) d\ell_A \\
 &\quad - \frac{\Gamma_{TE}}{j\omega 4\pi \epsilon_0} \int_{\ell_B} I_B^y d\ell_B \int_{\ell_A} d\ell_A \left[\frac{I_A^y}{R_2} \frac{\partial}{\partial R_2} \left(\frac{e^{-jk_1 R_2}}{R_2} \right) + \frac{R_y}{R_2} \right. \\
 &\quad \left. \cdot \frac{\partial}{\partial R_2} \left(\frac{1}{R_2} \frac{\partial}{\partial R_2} \left\{ \frac{e^{-jk_1 R_2}}{R_2} \right\} \right) (I_A^x R_x + I_A^y R_y + I_A^z R_z) \right] \quad (4.13)
 \end{aligned}$$

where $R_x = x_B - x'_A$; $R_y = y_B - y'_A$ and $R_z = z_B + z'_A$ and $R_2 = \sqrt{R_x^2 + R_y^2 + R_z^2}$.

The total mutual impedance between the two current elements becomes

$Z = Z^D + Z^I$, where Z^D is given by,

$$\begin{aligned}
 Z^D &= \frac{j\omega\mu_0}{4\pi} \int_{\ell_B} d\ell_B \int_{\ell_A} d\ell_A \vec{I}_A \cdot \vec{I}_B \frac{e^{-jk_1 R_1}}{R_1} \\
 &\quad + \frac{1}{j\omega 4\pi \epsilon_0} \int_{\ell_B} d\ell_B \int_{\ell_A} d\ell_A \frac{dI_A}{d\ell_A} \frac{dI_B}{d\ell_B} \frac{e^{-jk_1 R_1}}{R_1} \quad (4.14)
 \end{aligned}$$

where R_1 is given by (2.17).

A user-oriented computer program has been written [17,24] to solve for the current distribution and the field pattern of arbitrarily oriented wire antennas (this may include wire-junctions) over plane imperfect ground. Again the program follows directly from (4.13) and (4.14).

4.3. Validity of the Reflection-Coefficient Method as Compared with the Exact Solution

In general it is difficult to predict the accuracy of the so-called exact solution below a height of 0.03λ from the ground plane. If sections of the antenna structure below this height are all vertical then there are no difficulties but if there is any horizontal structure below a height 0.03λ then the method of integration used to integrate the semi-infinite integrals fails. It is safe to say that as long as there are no horizontal wire elements below a height of 0.03λ and as long as any structure below this height consists of all parallel vertical wires then the exact solution is valid.

For the reflection-coefficient method it is impossible to make any comment regarding accuracy for arbitrary structure. However, as long as the antenna structure is within the limits presented in the previous sections, it is possible to draw conclusions regarding its relative accuracy.

-
- [24] T. K. Sarkar, "Analysis of Radiation by Arrays of Arbitrarily Oriented Wire Antennas Over Plane Imperfect Ground (Reflection Coefficient Method)," IEEE Trans. Ant. and Propagat. (to be published).

4.4. Conclusion

Two user-oriented programs have been developed using both the Sommerfeld formulation and the reflection-coefficient method based on the analysis presented in the last section. The methods presented here and their corresponding programs handle arbitrary wire geometry including wire junctions and use piecewise linear functions to represent both I_A and I_B .

5. OPTIMIZATION METHODS FOR ARBITRARILY ORIENTED ARRAYS OF ANTENNAS OVER IMPERFECT GROUND

In this chapter methods are presented for optimizing certain performance indices of arbitrarily oriented arrays of wire antennas over imperfectly conducting ground. The indices considered include directivity, maximum power gain, quality factor, and the efficiency index sometimes referred as main-beam radiation efficiency. Optimization problems both with and without constraints on the resulting antenna pattern can be handled. In the first six sections attention is restricted to determine array feed voltages that will optimize some performance index. Strait and Kuo [25] presented the optimization methods for arrays of parallel vertical wire antennas in air. An attempt has been made to extend these methods for arbitrarily oriented structures now situated over imperfect ground. The next section deals with the optimization of certain performance indices as mentioned but this time with respect to the geometry of the antenna structure. This includes optimization with respect to spacing between elements, lengths of the elements and both lengths and spacings. Finally optimization of the indices with respect to loads applied at certain points on the antenna structure is also considered.

The problem of interest consists of an arbitrarily oriented antenna array of N -input ports plus a distant test antenna having one input port all situated over an imperfect ground plane. This is illustrated in Fig. 11. The array and the test antenna form an

-
- [25] B. J. Strait and D. C. Kuo, "Optimization Methods for Arrays of Parallel Wire Antennas," Scientific Report No. 18, Contract No. F19628-68-C-0180, AFCRL-72-0725, Syracuse University, Syracuse, New York: December 1972.

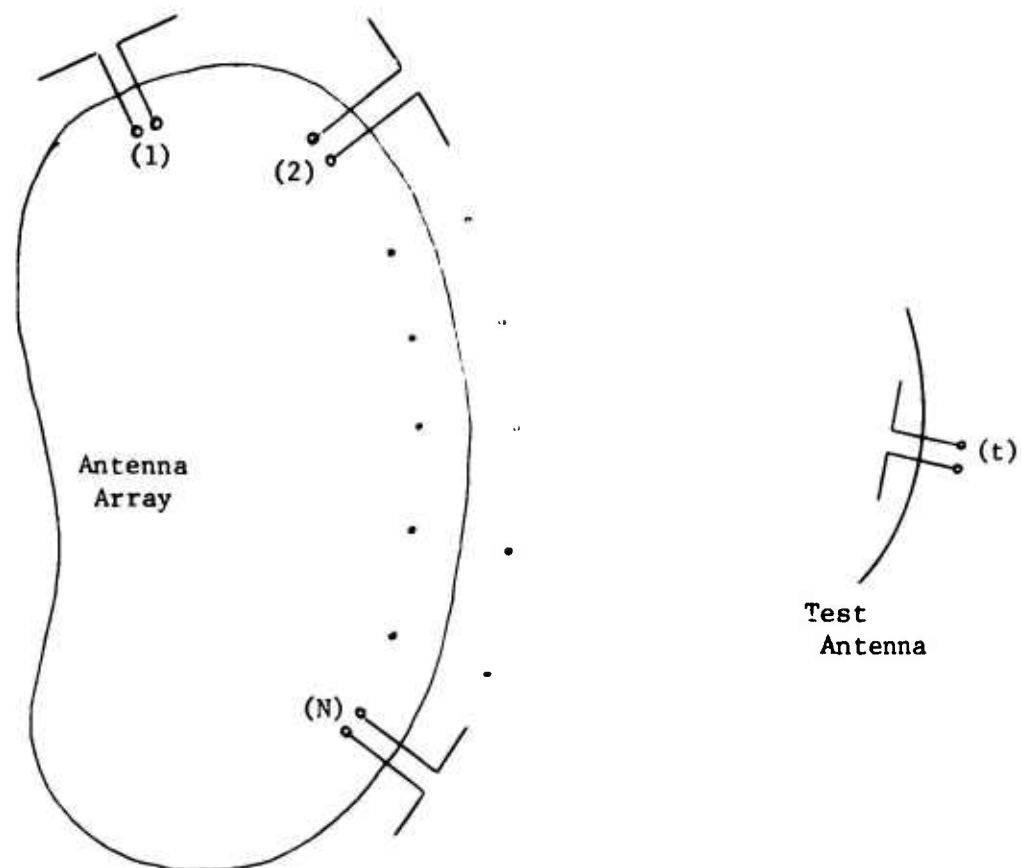


Fig. 11. Antenna array and distant test antenna.

(N+1)-port network whose terminal characteristics are determined by an (N+1) by (N+1) matrix. In order to obtain the terminal characteristics the antenna array is divided into subsections (as in the "Moment Method") and the current of the test antenna is represented by one expansion function only. The generalized impedance matrix is computed which completely characterizes the wire structure. Either the "exact" solution or the reflection-coefficient method is used to calculate individual matrix elements but one method is adhered to compute the whole matrix. The formulas presented in Chapters 2, 3 and 4 are utilized depending on the method used and the nature of the antenna structure. The impedance matrix is inverted to obtain the generalized admittance matrix $[Y]$ of the entire structure. The terminal admittance matrix $[Y]^T$ is obtained by retaining only those elements Y_{ij} for which both i, j represent the input ports of the antenna structure. So,

$$\begin{bmatrix} I_t \\ [I_a] \end{bmatrix} = \begin{bmatrix} Y_{tt} & [Y_{ta}] \\ [Y_{at}] & [Y_{aa}] \end{bmatrix} \begin{bmatrix} V_t \\ [V_a] \end{bmatrix} \quad (5.1)$$

where I_t , V_t and Y_{tt} are the terminal current, voltage and the input admittance of the test antenna, respectively. The corresponding terminal characteristics for the antenna array are expressed by the matrices $[I_a]_{N \times 1}$, $[V_a]_{N \times 1}$ and $[Y_{aa}]_{N \times N}$. $[Y_{ta}]_{1 \times N}$ and $[Y_{at}]_{N \times 1}$ represent the mutual admittances between the test antenna and the array ports incorporating the effects of the imperfect ground plane. Also $[Y_{aa}] = [\widetilde{Y}_{aa}]$ and $[Y_{ta}] = [\widetilde{Y}_{at}]$. Once the four admittance matrices of (5.1) are known array optimization problems can be handled as illustrated in the next sections.

5.1. Gain Maximization

The power gain for an antenna array is defined by

$$G = \frac{4\pi \times (\text{Radiation intensity for the specified direction})}{\text{Power input to the array}} \quad (5.2)$$

The power input to the array is given by

$$P_{in} = \frac{1}{2} [\widetilde{V}_a^*] \{ [Y_{aa}] + [\widetilde{Y}_{aa}^*] \} [V_a] \quad (5.3)$$

where * denotes complex conjugate and \sim denotes the transpose of the matrix. The test antenna is assumed to be appropriately polarized and located in the specific direction for which G is desired. It is also assumed that the test antenna is at a distance r from the array and situated in the far field. Under polarization-matched conditions, the square of the magnitude of the test antenna terminal current is proportional to the radiation intensity (R) of the incident field. For $V_t = 0$, the power received (P_r) is related to the gain (g) and the receiving aperture (A) of the test antenna by

$$\frac{R \times A \times g}{r^2} = |I_t|^2 R_{tt} \quad (5.4)$$

where R_{tt} is the input impedance of the test antenna. Since g, A and λ - the wavelength of propagation, are related by

$$A = \frac{\lambda^2 g}{4\pi} \quad (5.5)$$

it follows that

$$R = |I_t|^2 \frac{R_{tt} r^2 \lambda^2}{4\pi A^2} = |I_t|^2 \frac{K}{8\pi} \quad (5.6)$$

K is a constant which depends solely on the test antenna. Since

$I_t = [Y_{ta}][V_a]$ for $V_t = 0$, (5.6) can be expressed as

$$R = \frac{K}{8\pi} [\widetilde{V}_a^*] [\widetilde{Y}_{ta}^*] [Y_{ta}] [V_a] \quad (5.7)$$

Application of (5.3) and (5.7) to (5.2) yields

$$G = K \frac{[\tilde{V}_a^*] [\tilde{Y}_{ta}^*] [Y_{ta}] [V_a]}{[\tilde{V}_a^*] \{ [Y_{aa}] + [\tilde{Y}_{aa}^*] \} [V_a]} \quad (5.8)$$

The procedure for optimizing (5.8) for some specified direction is well-known [26]. This is a ratio of Hermitian quadratic forms, and it follows from the properties of these network matrices that $\{ [Y_{aa}] + [\tilde{Y}_{aa}^*] \}$ is positive definite while $[\tilde{Y}_{ta}^*] [Y_{ta}]$ is positive semidefinite. Hence all eigenvalues associated with the following equation

$$[\tilde{Y}_{ta}^*] [Y_{ta}] [V_a] = \frac{G}{K} \{ [Y_{aa}] + [\tilde{Y}_{aa}^*] \} [V_a] \quad (5.9)$$

are either zero or real and positive. Since $[\tilde{Y}_{ta}^*] [Y_{ta}]$ is a one-term dyad there is only one non-zero eigenvalue, and the corresponding eigenvector is found from

$$\frac{K}{G} \{ [Y_{aa}] + [\tilde{Y}_{aa}^*] \}^{-1} [\tilde{Y}_{ta}^*] [Y_{ta}] [V_a] = [V_a] \quad (5.10)$$

Since $[Y_{ta}] [V_a]$ is a scalar the excitation voltages required to maximize the gain in the specified direction are contained in the eigenvector

$$[V_a] = C \{ [Y_{aa}] + [\tilde{Y}_{aa}^*] \}^{-1} [\tilde{Y}_{ta}^*] \quad (5.11)$$

where C is a constant. Substitution of (5.11) to (5.10) yields

$$G_{\max} = K [Y_{ta}] \{ [Y_{aa}] + [\tilde{Y}_{aa}^*] \}^{-1} [\tilde{Y}_{ta}^*] \quad (5.12)$$

[26] R. F. Harrington, "Field Computation by Moment Methods," The Macmillan Company, New York, 1968.

Hence the voltages given by (5.11) (the constant C can be dropped with no effects on the result) can be used to maximize the gain of the array in the given direction. The result is G_{\max} given by (5.12).

5.2. Efficiency Indices

An efficiency index S (or inverse of sensitivity factor) sometimes called the main-beam radiation efficiency [27] has been defined for arrays of isotropic point sources as

$$S = \frac{(\text{radiation intensity corresponding to the direction of max. radiation})}{(\text{sum of the excitation current magnitudes squared})} \quad (5.13)$$

to serve as a measure or indication of the supergain condition. It has been pointed out [27] that superdirective arrays may require very large currents of opposite signs in neighboring elements, resulting in excessive heat loss and very low radiation intensity in the direction of the main beam. This generally undesirable condition is indicated by a relatively low value of S. The efficiency index has similar significance for arrays of electrically short wires. Use of (5.7) and $[I_a] = [Y_{aa}] [V_a]$ in (5.13) yields

$$S = \frac{K}{2} \frac{[\tilde{V}_a^*] [\tilde{Y}_{ta}^*] [Y_{ta}] [V_a]}{[\tilde{V}_a^*] [\tilde{Y}_{aa}^*] [Y_{aa}] [V_a]} \quad (5.14)$$

For longer wires it may be more useful to deal with either one of two possible alternative quantities that will also be labeled efficiency indices. One of these is obtained by using (5.13) with its denominator replaced by the sum of the excitation voltages squared. By denoting the resulting quantity by S_1 and use of (5.7) in (5.13) yields

[27] D. K. Cheng, "Optimization Techniques for Antenna Arrays," Proc. IEEE, No. 12, pp. 1664-1674, December 1971.

$$S_1 = \frac{K}{2} \frac{[\tilde{V}_a^*] [\tilde{Y}_{ta}^*] [Y_{ta}] [V_a]}{[\tilde{V}_a^*] [V_a]} \quad (5.15)$$

For longer wires a suitable alternative is obtained by using (5.13) with its denominator replaced by the sum of the current magnitudes squared over the entire array. The new efficiency index S_2 is then obtained as,

$$S_2 = \frac{K}{2} \frac{[\tilde{V}_a^*] [\tilde{Y}_{ta}^*] [Y_{ta}] [V_a]}{[\tilde{V}_a^*] [\tilde{Y}^*] [Y] [V_a]} \quad (5.16)$$

where the admittance matrix $[Y]$ is obtained by retaining only those columns of $[Y]$ which correspond to the input ports of the antenna array.

The excitation voltages that will maximize the efficiency indices S , S_1 and S_2 can be obtained from the method of Section 5.1. Results are

$$S_{\max} = \frac{K}{2} [Y_{ta}] \{ [\tilde{Y}_{aa}^*] [Y_{aa}] \}^{-1} [\tilde{Y}_{ta}^*] \quad (5.17)$$

corresponding to the feed voltages given by (within an arbitrary constant)

$$[V_a] = \{ [\tilde{Y}_{aa}^*] [Y_{aa}] \}^{-1} [\tilde{Y}_{ta}^*] \quad (5.18)$$

Also,

$$(S_1)_{\max} = \frac{K}{2} [Y_{ta}] [\tilde{Y}_{ta}^*] \quad (5.19)$$

with feed voltages given by

$$[V_a] = [\tilde{Y}_{ta}^*] \quad (5.20)$$

Finally

$$(S_2)_{\max} = \frac{K}{2} [Y_{ta}] \{ [\tilde{Y}^*] [Y] \}^{-1} [\tilde{Y}_{ta}^*] \quad (5.21)$$

resulting from feed voltages given by

$$[V_a] = \{ [\tilde{Y}_{aa}^*] [Y_{aa}] \}^{-1} [\tilde{Y}_{ta}^*] \quad (5.22)$$

Thus the three choices for efficiency index can be calculated for any arbitrarily oriented antenna array over an imperfect ground plane by using the formulas for impedances described in Chapters 2, 3 and 4.

5.3. Quality Factor

A quality factor can be defined for arbitrarily oriented arrays over imperfect ground that relates gain and efficiency index. For arrays of electrically short wires it is convenient to use the quality factor Q defined for arrays of isotropic point sources as

$$Q = \frac{4\pi (\text{sum of excitation currents squared})}{\text{power input to the array}} \quad (5.23)$$

So that from (5.2), (5.13) and (5.23)

$$G = QS \quad (5.24)$$

Application of (5.3) and $[I_a] = [Y_{aa}] [V_a]$ in (5.23) yields

$$Q = \frac{8\pi [\tilde{V}_a^*] [\tilde{Y}_{aa}^*] [Y_{aa}] [V_a]}{[\tilde{V}_a^*] \{ [Y_{aa}] + [\tilde{Y}_{aa}^*] \} [V_a]} \quad (5.25)$$

Similarly, alternative quality factors Q_1 and Q_2 are defined corresponding to the efficiency indices of (5.15) and (5.16). The result is that (5.24) holds with the product QS replaced by $Q_1 S_1$ or $Q_2 S_2$, which ever is appropriate. By using the equivalent of (5.24), then it is obvious that

$$Q_1 = \frac{8\pi [\tilde{V}_a^*] [V_a]}{[\tilde{V}_a^*] \{ [Y_{aa}] + [\tilde{Y}_{aa}^*] \} [V_a]} \quad (5.26)$$

and

$$Q_2 = \frac{8\pi [\widetilde{V}_a^*] [\widetilde{Y}^*] [Y] [V_a]}{[\widetilde{V}_a^*] \{ [Y_{aa}] + [\widetilde{Y}_{aa}^*] \} [V_a]} \quad (5.27)$$

Hence the quality factors Q , Q_1 and Q_2 can be computed once the antenna structure and the feed voltages are known. These quantities can be optimized by a procedure as outlined in the previous section.

5.4. Optimization Subject to Constraints on Pattern Nulls in the Upper Half-Space

The problem of optimizing the directivity or any of the efficiency indices subject to constraints on the resulting pattern nulls in the upper half-space is discussed in this section. The field pattern in a certain direction above the ground plane for an arbitrarily oriented antenna array over imperfect ground will be proportional to $|I_t|$, where I_t is the short-circuit current flowing through the test dipole located in that particular direction. Specifically the field (E^p) in direction p above ground is related to the short-circuit current I_t^p in the test dipole which is located in the p -direction by

$$|E_t^p| = \sqrt{2\eta R_{tt}} |I_t^p| \quad (5.28)$$

where η and R_{tt} are the wave impedance and input resistance of the test dipole respectively. The problem is to determine the feed voltages that will provide pattern nulls in p specified directions in the upper half-space and a maximum of one of the performance indices (say the gain) in a given $(p+1)$ direction subject to these constraints. An equation relating the short circuit current in the test dipole for each of the $(p+1)$ directions to the admittance matrix and the feed voltages can be written as follows:

$$\begin{bmatrix} I_t^1 \\ I_t^2 \\ \vdots \\ I_t^p \\ I_t^{p+1} \end{bmatrix}_{(p+1) \times 1} = \begin{bmatrix} 0 \\ 0 \\ \vdots \\ 0 \\ I_t \end{bmatrix}_{(p+1) \times 1} = \begin{bmatrix} [Y_t^1]_{1 \times N} \\ [Y_t^2]_{1 \times N} \\ \vdots \\ [Y_t^p]_{1 \times N} \\ [Y_t^{p+1}]_{1 \times N} \end{bmatrix}_{(p+1) \times N} \begin{bmatrix} [V_a] \end{bmatrix}_{N \times 1} \quad (5.29)$$

where the matrix $[Y_t^p]$ is the transfer admittance matrix between the test dipole in the p-direction and the excited ports of the antenna array, taking into account the effects of the imperfect ground plane. $\sqrt{2\eta R_{tt}} |I_t^p|$ is then the field in the direction designated for the maximum performance index. Equation (5.29) can be portioned in the following form

$$\begin{bmatrix} [0] \\ I_t \end{bmatrix} = \begin{bmatrix} [Y_t^{11}]_{p \times p} & [Y_t^{12}]_{p \times (N-p)} \\ [Y_t^{21}]_{1 \times p} & [Y_t^{22}]_{1 \times (N-p)} \end{bmatrix} \begin{bmatrix} [V_a^1]_{p \times 1} \\ [V_a^2]_{(N-p) \times 1} \end{bmatrix} \quad (5.30)$$

Hence

$$[V_a^1] = - [Y_t^{11}]^{-1} [Y_t^{12}] [V_a^2] \triangleq [B] [V_a^2] \quad (5.31)$$

and

$$I_t = \{ [Y_t^{21}] [B] + [Y_t^{22}] \} [V_a^2] \triangleq [C] [V_a^2] \quad (5.32)$$

If the performance index chosen to be maximized is the gain then from (5.2), (5.6) and (5.32)

$$G = \frac{K}{2} \frac{[V_a^{2*}] [\tilde{C}^*] [C] [V_a^2]}{P_{in}} \quad (5.33)$$

and P_{in} from (5.3) is given as

$$P_{in} = \frac{1}{2} [\widetilde{V}_a^*] \{ [Y_{aa}] + [\widetilde{Y}_{aa}^*] \} [V_a]$$

and with $[V_a]$ written in partitioned form

$$P_{in} = \frac{1}{2} \left\{ \begin{bmatrix} [\widetilde{V}_a^{1*}] \\ [\widetilde{V}_a^{2*}] \end{bmatrix} \right\} \{ [Y_{aa}] + [\widetilde{Y}_{aa}^*] \} \begin{bmatrix} [V_a^1] \\ [V_a^2] \end{bmatrix} \quad (5.34)$$

Application of (5.31) leads to

$$P_{in} = \frac{1}{2} [\widetilde{V}_a^{2*}] \left\{ \begin{bmatrix} [\widetilde{B}^*] \\ [U] \end{bmatrix} \right\} \{ [Y_{aa}] + [\widetilde{Y}_{aa}^*] \} \begin{bmatrix} [B] \\ [U] \end{bmatrix} [V_a^2]$$

or

$$P_{in} \triangleq \frac{1}{2} [\widetilde{V}_a^{2*}] [Q] [V_a^2] \quad (5.35)$$

where $[U]$ is a unit matrix and $[Q]$ is defined by (5.34) and (5.35).

Hence, application of (5.35) to (5.33) yields

$$G = K \frac{[\widetilde{V}_a^{2*}] [\widetilde{C}^*] [C] [V_a^2]}{[\widetilde{V}_a^{2*}] [Q] [V_a^2]} \quad (5.36)$$

Once again (5.36) is a ratio of Hermitian forms with $[Q]$ positive definite and $[\widetilde{C}^*] [C]$ positive semidefinite. Furthermore the latter is a one term dyad so that the procedure for maximizing the gain is identical to that used in Section 5.1. The results are

$$G_{max} = K \cdot [C] [Q]^{-1} [\widetilde{C}^*] \quad (5.37)$$

and

$$[V_a^2] = [Q]^{-1} [\widetilde{C}^*] \quad (5.38)$$

Once $[V_a^2]$ is known $[V_a^1]$ can be obtained from (5.31) which completes the solution. If no pattern constraints are used then (5.37) and (5.38) reduce to the solution of Section 5.1.

The procedure for optimizing any of the efficiency indices defined in Section 5.2 subject to constraints on the resulting pattern nulls in the upper half-space follows exactly the same procedure.

5.5. Optimization Subject to Constraints on the Resulting Sidelobes in the Upper Half Space

Next, the problem of finding excitation voltages that will maximize a performance index (of an arbitrarily oriented antenna structure over an imperfect ground plane) in a given direction subject to constraints on the resulting sidelobe levels is considered. Suppose I_t^0 denotes the short circuit current in a small test antenna located in a direction corresponding to the direction designated for a maximum of a given performance index (say gain), and $I_t^1, I_t^2, \dots, I_t^p$ denote values of the short circuit current, induced in small fast antennas located in direction, corresponding to the peaks of the p sidelobes to be constrained in the pattern. The short-circuit currents in the test antennas are proportional to the field intensities in those directions and are related by (5.28). Using partitioned matrices

$$\begin{bmatrix} I_t^0 \\ I_t^1 \\ \vdots \\ I_t^p \end{bmatrix} = \begin{bmatrix} [Y_t^{AA}]_{1 \times (N-p)} & [Y_t^{AB}]_{1 \times p} \\ \vdots & \vdots \\ [Y_t^{BA}]_{p \times (N-p)} & [Y_t^{BB}]_{p \times p} \end{bmatrix} \begin{bmatrix} [V_a^A]_{(N-p) \times 1} \\ [V_a^B]_{p \times 1} \end{bmatrix} \quad (5.39)$$

Assuming $[Y_t^{BB}]$ to be nonsingular

$$[V_a^B] = [Y_t^{BB}]^{-1} \left[\begin{bmatrix} I_t^1 \\ \vdots \\ I_t^p \end{bmatrix} - [Y_t^{BA}] [V_a^A] \right] \quad (5.40)$$

An alternative to (5.40) is possible if it is not required to satisfy (5.39) exactly. That is, if a least squares solution is acceptable it is possible to use less than p voltages in $[V_a^B]$. That is, $[V_a^B]$ and $[V_a^A]$ are of dimensions m and $N-m$ respectively where $m < p$, then the dimensions of the other matrices change accordingly with $[Y_t^{BB}]$ no longer square. A least squares solution is then obtained using

$$[V_a^B] = \{ [\widetilde{Y_t^{BB}}]^* [Y_t^{BB}] \}^{-1} [\widetilde{Y_t^{BB}}]^* \begin{bmatrix} 1 \\ I_t^1 \\ \vdots \\ I_t^p \end{bmatrix} - [Y_t^{BA}] [V_a^A] \quad (5.41)$$

in place of (5.40)

Using a suggestion of Sanzgiri and Butler [28] the short-circuit current in the test dipole corresponding to the peak of the i th sidelobe can be denoted by $I_t^1 = e_i I_t^0$ so that

$$\begin{bmatrix} I_t^1 \\ \vdots \\ I_t^p \end{bmatrix} = \begin{bmatrix} e_1 I_t^0 \\ \vdots \\ e_p I_t^0 \end{bmatrix} \triangleq [E] I_t^0 \quad (5.42)$$

Then, from (5.38)

$$I_t^0 = \frac{1}{\psi} [F] [V_a^A] \quad (5.43)$$

where

$$\psi = 1 - [Y_t^{AB}] [Y_t^{BB}]^{-1} [E] \quad (5.44)$$

and

$$[F] = [Y_t^{AA}] - [Y_t^{AB}] [Y_t^{BB}]^{-1} [Y_t^{BA}] \quad (5.45)$$

[28] S. M. Sanzgiri and J. K. Butler, "Constrained Optimization of the Performance Indices of Arbitrary Array Antennas," IEEE Transactions on Antennas and Propagation, Vol. AP-19, No. 4, pp. 493-498, July 1971.

The input power is given by (5.34) and using (5.40) and (5.42) - (5.45) in (5.34) results in

$$P_{in} = \frac{1}{2} [\tilde{V}_a^{A*}] [Q'] [V_a^A] \quad (5.46)$$

where in this case

$$[Q'] = \{ [U] \} \{ [\tilde{G}^*] \} \{ [Y_{aa}] + [\tilde{Y}_{aa}^*] \} \begin{bmatrix} [U] \\ [G] \end{bmatrix} \quad (5.47)$$

and

$$[G] = \frac{1}{\psi} [Y_t^{BB}]^{-1} \{ [E] [F] - \psi [Y_t^{BA}] \} \quad (5.48)$$

Of course (5.44), (5.45), (5.47) and (5.48) must be changed appropriately, if (5.41) is used rather than (5.40).

If the performance index to be maximized is chosen again to be gain then,

$$G = K \frac{[\tilde{V}_a^{A*}] [\tilde{F}^*] [F] [V_a^A]}{[\tilde{V}_a^{A*}] [Q'] [V_a^A]} \quad (5.49)$$

The matrix $[\tilde{F}^*] [F]$ is a one term dyad and the procedure for optimizing (5.49) is again that of Section 5.1. The results are

$$G_{max} = \frac{K}{|\psi|^2} [F][Q']^{-1} [\tilde{F}^*] \quad (5.50)$$

$$[V_a^A] = [Q']^{-1} [\tilde{F}^*] \quad (5.51)$$

$$[V_a^B] = [G] [V_a^A] \quad (5.52)$$

The iterative optimization procedure is then simply to guess the initial sidelobe directions and compute the matrices necessary to determine G_{max} and the required voltages (5.50) to (5.54). The resulting sidelobe directions and peaks are then computed and compared with desired results.

The new sidelobe directions are used, of course, as "initial guesses" for the next iteration. The iterative procedure is continued until the levels of all sidelobes to be constrained are within some prescribed tolerance.

Obviously, constrained optimization of the various efficiency indices defined earlier can be carried out in the same way.

5.6. Optimization of One Performance Index Subject to a Constraint on Another

A procedure for optimizing a given performance index (of an arbitrarily oriented antenna array over an imperfect ground plane) subject to a constraint on another performance index is outlined here. In this discussion an index denoted by

$$\frac{\tilde{[V_a^*]} [R_1] [V_a]}{\tilde{[V_a^*]} [R_2] [V_a]}$$

will be optimized subject to the constraint given by

$$\frac{\tilde{[V_a^*]} [R_3] [V_a]}{\tilde{[V_a^*]} [R_4] [V_a]} = \gamma \text{ (a given constant).} \quad (5.53)$$

Once the performance indices are specified $[R_1]$, $[R_2]$, $[R_3]$ and $[R_4]$ have precise meanings. A solution is obtained by setting

$$L = \frac{\tilde{[V_a^*]} [R_1] [V_a]}{\tilde{[V_a^*]} [R_2] [V_a]} + \lambda \left\{ \frac{\tilde{[V_a^*]} [R_3] [V_a]}{\tilde{[V_a^*]} [R_4] [V_a]} - \gamma \right\} \quad (5.54)$$

stationary with respect to the column vector $[V_a]$ and the Lagrangian multiplier λ . Setting the first variation of L with respect to $[V_a]$ equal to zero yields

$$[V_a] = a [H]^{-1} [\tilde{S}_1^*] \quad (5.55)$$

where a is a constant given by

$$a = \{[S_1] [V_a]\} \{[\tilde{V}_a^*] [R_2] [V_a]\} \{[\tilde{V}_a^*] [R_1] [V_a]\}^{-1} \quad (5.56)$$

and

$$[R_1] = [\tilde{S}_1^*] [S_1]$$

The matrix $[H]$ is given by

$$[H] = [R_2] + \gamma b [R_4] - b [R_3] \quad (5.57)$$

where the constant b is

$$b = \lambda \{[\tilde{V}_a^*] [R_4] [V_a]\}^{-1} \{[\tilde{V}_a^*] [R_2] [V_a]\}^2 \{[\tilde{V}_a^*] [R_1] [V_a]\}^{-1} \quad (5.58)$$

The results are essentially those obtained by Lo, Lee and Lee [29] for the special case when $[R_3]$ is a unit matrix; although of course, not only mutual coupling is incorporated in the matrices dealt with here, but also the effects of the imperfect ground.

When (5.55) is substituted in the constraint equation (5.53) it follows that

$$[S_1] \{[H]^{-1} (\gamma [R_4] - [R_3]) [H]^{-1} [\tilde{S}_1^*]\} = 0 \quad (5.59)$$

where it is assumed that $[R_1]$, $[R_2]$, $[R_3]$, $[R_4]$ and $[H]$ are Hermitian. The only unknown in (5.59) is b which is contained in matrix $[H]$.

The procedure for finding b is spelled out by Winkler and Schwartz [30]. It is evident from (5.59) that the column vector shown in brackets

- [29] Y. T. Lo, S. W. Lee and D. H. Lee, "Optimization of Directivity and Signal to Noise Ratio of an Arbitrary Antenna Array," Proc. IEEE, Vol. 54, No. 8, pp. 1033-1045, August 1966.
- [30] L. P. Winkler and M. Schwartz, "A Fast Numerical Method for Determining the Optimum SNR of an Array Subject to a Q-Factor Constraint," IEEE Transaction on Antennas and Propagation, Vol. AP-20, No. 4, pp. 503-505, July 1972.

is orthogonal to $[S_1]$. It follows that a complete set $\{[f_n]\}$ can be constructed with $[S_1]$ as one of its elements. If $[S_1]$ is written as

$$[S_1] = [s_1, s_2, s_3, \dots, s_N] \quad (5.60)$$

where N is the number of independent applied excitations then

$$\begin{aligned} [f_1] &= [s_1, s_2, s_3, s_4, \dots, s_N] \\ [f_2] &= \left[\frac{-1}{s_1}, \frac{1}{s_2}, 0, 0, \dots, 0 \right] \\ [f_3] &= \left[-\frac{1}{s_1}, 0, \frac{1}{s_3}, 0, \dots, 0 \right] \\ &\vdots \\ [f_N] &= \left[-\frac{1}{s_1}, 0, 0, 0, \dots, \frac{1}{s_N} \right] \end{aligned} \quad (5.61)$$

forms a complete independent set with $[f_1]$ orthogonal to all others. The bracketed column vector in (5.59) can then be expressed as a linear combination of $[f_i]$ written as

$$[H]^{-1} (\gamma[R_4] - [R_3]) [H]^{-1} [\tilde{S}_1^*] = \sum_{i=2}^N q_i [\tilde{f}_i] \quad (5.62)$$

This is easily arranged as

$$[W] [\tilde{Q}] = 0 \quad (5.63)$$

where

$$[Q] = [-1, q_2, q_3, \dots, q_N] \quad (5.64)$$

and $[W]$ is a matrix with columns $[W_i]$ given by

$$[W_1] = [\tilde{f}_1^*] = [\tilde{S}_1^*] \quad (5.65)$$

$$\begin{aligned} [W_i] &= h^2 (\gamma[R_4] - [R_3]) [\tilde{f}_i] + 2h[R_2][\tilde{f}_i] \\ &\quad + [R_2] (\gamma[R_4] - [R_3])^{-1} [R_2] [\tilde{f}_i] \\ &\quad \text{for } i = 2, 3, 4, \dots, N \end{aligned} \quad (5.66)$$

Rewriting (5.63) in terms of its real and imaginary parts in the form

$$\begin{bmatrix} W_{11r} - W_{11i} & W_{12r} - W_{12i} & \dots \\ W_{11i} - W_{11r} & W_{12i} & W_{12r} & \dots \\ W_{21r} - W_{21i} & & & \\ W_{21i} - W_{21r} & & & \end{bmatrix} \begin{bmatrix} q_{1r} \\ q_{1i} \\ q_{2r} \\ q_{2i} \\ \vdots \end{bmatrix} = \begin{bmatrix} 0 \\ 0 \\ 0 \\ \vdots \end{bmatrix} \quad (5.67)$$

or $[W'] [\tilde{Q}'] = 0 \quad (5.68)$

where $[W']$ is a square matrix of dimension twice that of $[W]$, and $[\tilde{Q}']$ is a column vector of dimension twice that of $[Q]$. By using (5.66), (5.68) can be rewritten

$$\{b^2 [A_1] + b [A_2] + [A_3]\} [\tilde{Q}'] = 0 \quad (5.69)$$

where $[A_1]$ and $[A_2]$ are $2N \times 2N$ singular matrices (their first two columns are zero) and $[A_3]$ is a $2N \times 2N$ invertible matrix. Then from (5.69) Winkler and Schwartz [30] show that values of b can be found by determining the real eigenvalues of

$$[G] [X] = \frac{1}{b} [X] \quad (5.70)$$

where $[G]$ is an unsymmetric matrix given by

$$[G] = \begin{bmatrix} [0] & [U] \\ -[A_3]^{-1} [A_1] & -[A_3]^{-1} [A_2] \end{bmatrix}_{4N \times 4N} \quad (5.71)$$

where $[U]$ is a unit matrix.

For each real value of b one set of excitation voltages is computed using (5.55). Each of these sets is then used to compute corresponding values of both the constrained index and the index to be optimized. The set finally chosen is the one which yields the optimum result subject to the correct constraint.

5.7. Optimization with Respect to Antenna Geometry

With an appropriate optimization procedure, the performance indices presented in the previous sections may be maximized through adjustments of the antenna structure. In this case either lengths, spacings or both lengths and spacings are to be determined so as to maximize a performance index given by either (5.8), (5.14), (5.15), (5.16), (5.25), (5.26) or (5.27). The starting point in the optimization procedure can be an initial state corresponding to some classical or other improved design procedure. At each refinement, the admittance matrices $[Y_{ta}]$ and $[Y_{aa}]$ are recomputed and the performance index is calculated by the optimization procedure till the design parameters meet certain error specifications.

The next problem is to reduce the sidelobe levels below a certain level of an antenna array over an imperfect ground plane by adjusting the antenna geometry. Since the electric field in the upper half space in a certain direction is related to the short circuit current I_t in the test dipole by (5.28), an error criterion can be defined as

$$r = \sum_{i=1}^n \left| |I_t^i|^2 - |I_t|^2 \right| \quad \text{for } |I_t^i| > |I_t|$$

$$= 0 \quad \text{for } |I_t^i| < |I_t|$$

where I_c^i is the value of the short circuit current in the test dipole oriented in the i -th direction and n is the number of the observations calculated over the sidelobe region of the pattern. Of course, the error criterion ϵ is the quantity to be minimized as the optimization procedure progresses. Since at each optimization step the admittance matrices $[Y_{ta}]$ and $[Y_{aa}]$ are recomputed this is indeed a very time-consuming process. These types of optimizations have been done for parallel vertical wires in echelon [31], and could easily be extended to arrays of arbitrarily oriented wires over imperfect ground provided, of course, that sufficient computer time is available.

5.8. Optimizations of Loaded Antennas

In this problem (as in the previous) one has to recompute the admittance matrices $[Y_{ta}]$ and $[Y_{aa}]$ at each optimization step. The problem in this case involves optimization of the loads that are applied either at some specific points or distributed along a section of the arbitrarily oriented antenna structure. Once the total impedance matrix $[Z]_s$ for the entire structure has been computed excluding the loads (but including the effects of the imperfect ground plane) the effect of the loads can be taken into account by adding a load impedance matrix $[Z]_l$ to $[Z]_s$. This load impedance matrix is a square matrix having the same number of columns as $[Z]_s$, where the number equals the number of segments into which the N -port antenna array has been divided. For passive point-by-point loading $[Z]_l$ is a diagonal matrix having a zero on the diagonal

-
- [31] B. J. Strait, T. K. Sarkar and D. C. Kuo, "Special Programs for Analysis of Radiation by Wire Antennas," on Contract F19628-73-C-0047, AFCRL-73-0399, Syracuse University, Syracuse, NY 13210.

corresponding to each unloaded triangle function. Thus if there is a lumped load of Z_{ln} ohms at a wire position corresponding to the peak of the n th triangle function, then the element corresponding to the n th row and column of the diagonal matrix $[Z]_l$ is Z_{ln} . Thus the total impedance matrix $[Z]_T$ comprising of the loaded antenna structure over the plane imperfect ground is then

$$[Z]_T = [Z]_s + [Z]_l$$

In this case the terminal admittance matrix $[Y]_{sl}^T$ is obtained by retaining only those elements $\{[Z]_T^{-1}\}_{ij}$ which correspond to the excitation ports of the antenna structure. Hence once $[Y_{ta}]_{sl}$ and $[Y_{aa}]_{sl}$ are obtained the performance indices given by either (5.8), (5.14), (5.15), (5.16), (5.25), (5.26) or (5.27) can be easily computed. An optimization procedure now can be used with an initial guess to optimize the performance index with respect to the loads Z_{ln} . The starting point for the iterative procedure is the unloaded structure. The final result is a structure loaded at n -points by $[Z_{ln}]$ which optimize the required performance index.

The same procedure can again be applied to reduce sidelobes of the fields in the upper half space by application of loading to antenna structure. As described in the previous section, the same error criterion is defined but the parameters to be optimized are not the structure over the plane imperfect ground. The starting point for the iterative procedure is the pattern in the upper half space of an unloaded antenna geometry. The final result is the same array over the plane imperfect ground but loaded and having sidelobe near the desired level in the upper half space.

6. CONCLUSION

The mathematical foundations for newly developed user-oriented computer programs have been presented and described for handling arbitrarily oriented thin-wire antennas radiating in the presence of a plane imperfect ground. Properties of the imperfect ground are taken into account either exactly by using the Sommerfeld formulation or approximately by using the reflection-coefficient method. Application of interpolatory quadrature formulas to integrate the semi-infinite integrals encountered in the exact Sommerfeld formulation has reduced the time of computation as compared with other available procedures. A modified method of steepest descent has been used to evaluate the semi-infinite integrals to reduce required computing time without significant loss of accuracy. The commonly used reflection-coefficient method is derived in detail and its relative accuracy is discussed.

Methods have been presented for optimizing various performance indices of arbitrarily oriented thin-wire antennas over plane earth ground. Performance indices considered include directivity, maximum power gain, quality factor and efficiency index. It has been shown how a performance index can be optimized subject either to constraints on the directions of nulls in the resulting pattern or to constraints on the levels of the resulting sidelobes. It has also been shown how one performance index can be optimized subject to a constraint on another. The methods presented are quite general in that the wires can be excited or loaded at arbitrary points along their lengths.

In summary the contributions presented in this thesis include the following:

- 1) Application of interpolatory quadrature formulas to integrate the semi-infinite integrals encountered in the exact Sommerfeld formulation was illustrated.
- 2) Use of a modified method of steepest descent to evaluate the semi-infinite integrals to reduce the time of computation without significant loss of accuracy has been demonstrated.
- 3) The commonly used reflection-coefficient method was derived in detail and its relative accuracy was discussed.
- 4) New, user-oriented computer programs for treating the imperfect ground problem have been developed and described.
- 5) Formulas and results convenient for application to optimization and design problems have been presented.

Appendix A. QUADRATURES OF THE HIGHEST ALGEBRAIC ACCURACY

Certain integrals of the type $\int_a^h f(x)dx$ and $\int_0^\infty F(x)dx$ have been encountered in the course of this work. A method for evaluating these types of integrals very efficiently is discussed here. The following subject matter has been summarized from Krylov [33] to illustrate the salient features of this technique.

Because of its geometrical interpretation the problem of finding the numerical value of an integral of a function of one variable is often for simplicity called quadrature. One method of quadrature used is to evaluate integrals approximately by means of a finite number of values of the integrand. In many cases this method requires less work than other quadrature methods.

Quadrature formulas are often constructed from interpolating polynomials. In this way we can, in many cases, obtain quadrature formulas which are convenient to use and which will give sufficiently accurate results. For n arbitrary points x_1, x_2, \dots, x_n in the segment $[a, b]$, we can construct the interpolating polynomial for $f(x)$ by the following formulas

$$f(x) = P(x) + r(x) \quad (\text{A.1})$$

$$P(x) = \sum_{k=1}^n \frac{W(x)}{(x-x_k) W'(x_k)} f(x_k) \quad (\text{A.2})$$

$$W(x) = (x-x_1)(x-x_2) \dots (x-x_n) \quad (\text{A.3})$$

$$r(x) = \text{remainder of interpolation} \quad (\text{A.4})$$

[33] V. I. Krylov, "Approximate Calculations of Integrals," Macmillan Company, New York, 1962.

The exact value of the integral $\int_a^b p(x) f(x) dx$ is

$$\int_a^b p(x) f(x) dx = \int_a^b p(x) P(x) dx + \int_a^b p(x) r(x) dx \quad (\text{A.5})$$

where $p(x)$ is the weight function. It is assumed that $p(x)$ is a certain fixed function, which is measurable on $[a, b]$ and is not identically the zero function, and that the product $p(x)f(x)$ is integrable on $[a, b]$. If the interpolation (A.1) is sufficiently accurate so that the remainder $r(x)$ is small throughout the interval $[a, b]$ then the second term in (A.5) can be neglected and the approximate equation obtained is

$$\int_a^b p(x) f(x) dx \approx \sum_{k=1}^n A_k f(x_k) \quad (\text{A.6})$$

where

$$A_k = \int_a^b p(x) \frac{W(x)}{(x-x_k) W'(x_k)} dx \quad (\text{A.7})$$

Quadrature formulas for which the coefficients have the form (A.7) are called interpolatory quadrature formulas. Interpolatory quadrature formulas can be characterized by the following theorem.

Theorem 1: In order that the quadrature formula be interpolatory it is necessary and sufficient that it be exact for all possible polynomials of degree $\leq n-1$.

$$\text{The quadrature formula } \int_a^b p(x) f(x) dx \approx \sum_{k=1}^n A_k f(x_k) \text{ for a fixed } n,$$

contains $2n$ parameters A_k and x_k ($k=1, 2, \dots, n$). The problem is to select these parameters so that (A.6) will be exact for all polynomials of the highest degree (i.e. for all polynomials of degree $\leq k$, where k is as

large as possible). The choice of the coefficients A_k for any arrangement of x_k can lead to an equation (A.6) which is exact for all polynomials of degree $\leq n-1$. This requirement completely defines the coefficients A_k : (A.6) must be interpolatory and its coefficients must be given by (A.7)

In order to increase the precision of (A.6) the choice of the points x_k is still at our disposal. We might hope that for some choice of these points the degree of precision can be increased by n and that the formula can be made exact for all polynomials of degree $\leq 2n-1$. This can be achieved as shown below. The conditions which must be satisfied by A_k and x_k in order that (A.6) will be exact will now be established.

We prefer to consider the polynomial $W(x) = (x-x_1)(x-x_2)\dots(x-x_n)$ instead of the nodes x_k themselves. If we know the x_k , then we can easily construct the polynomial $W(x)$. Conversely, if we know the polynomial $W(x) = x^n + a_1x^{n-1} + \dots$, then determining the roots of $W(x)$ will give us the x_k . If we determine $W(x)$ instead of x_k directly then we must be careful that the roots of $W(x)$ will be real, distinct and located in the segment $[a, b]$.

Theorem 2: If (A.6) is to be exact for all polynomials of degree $\leq (2n-1)$, then it is necessary and sufficient that (A.6) must be interpolatory and that the polynomial $W(x)$ be orthogonal with respect to $p(x)$ to all polynomials $Q(x)$ of degree $< n$:

$$\int_a^b p(x) W(x) Q(x) dx = 0 \quad (\text{A.8})$$

The possibility of constructing formulas which are exact for all polynomials of degree $2n-1$ is related to the existence of polynomials $W(x)$ of degree n which possess the above orthogonality property. If the weight function $p(x)$ changes sign on $[a,b]$ then such a polynomial $W(x)$ may not exist. If such a polynomial does exist its roots might not satisfy the above requirements. Hence it will be assumed that the weight function $p(x)$ is nonnegative on $[a,b]$.

Theorem 3: If the polynomial $P_n(x)$ is orthogonal on the segment $[a,b]$ to all polynomials of degree less than n , with respect to a nonnegative weight function $p(x)$, then all the roots of $P_n(x)$ are real, distinct and lie inside $[a,b]$.

Theorem 4: If $p(x) > 0$ for $x \in [a,b]$, then a quadrature formula (A.6) which is exact for all polynomials of degree $\leq 2n-1$, exists for all n , and cannot be exact for all polynomials of degree $2n$.

The construction of quadrature formulas which have the highest accuracy is now discussed. Consider the system of polynomials $P_n(x)$; ($n=1,2,\dots$) which are orthogonal on $[a,b]$ with respect to the weight function $p(x)$. In order to be definite, it is assumed that the system is normalized,

$$\int_a^b p(x) P_n(x) P_m(x) dx = \begin{cases} 0 & \text{for } m \neq n \\ 1 & \text{for } m = n \end{cases} \quad (\text{A.9})$$

and the n th degree polynomial of an orthonormal system can be assumed to be of the form

$$P_n(x) = a_n x^n + b_n x^{n-1} + \dots$$

The n th degree polynomial of this system then differs from $W(x)$ by only a constant multiple. The roots of $P_n(x)$ will thus be the nodes x_k ($k = 1, 2, \dots, n$) which are to be used in the quadrature formula. The coefficients A_k are determined by (A.7) or equivalently by,

$$A_k = \int_a^b p(x) \frac{P_n(x)}{(x-x_k) P_n'(x)} dx \quad (A.10)$$

In order to calculate A_k by (A.10) the Christoffel Darboux identity is used. Three consecutive polynomials of an orthonormal set satisfy a recursion relation

$$xP_n(x) = \frac{a_n}{a_{n+1}} P_{n+1}(x) + \left(\frac{b}{a_n} - \frac{b_{n+1}}{a_{n+1}}\right) P_n(x) + \frac{a_{n-1}}{a_n} P_{n-1}(x) \quad (A.11)$$

from which the Christoffel-Darboux identity can be deduced

$$(x-t) \sum_{k=0}^n P_k(x) P_k(t) = \frac{a_n}{a_{n+1}} [P_{n+1}(x) P_n(t) - P_n(x) P_{n+1}(t)] \quad (A.12)$$

From (A.12) it can be written that

$$A_k = - \frac{a_{n+1}}{a_n} \frac{1}{P_n'(x_k) P_{n+1}(x_k)} = \frac{a_n}{a_{n-1}} \frac{1}{P_n'(x_k) P_{n-1}(x_k)} \quad (A.13)$$

Thus from the second equality of (A.13) it is clear that a quadrature formula of the highest accuracy has all positive coefficients.

Next the magnitude of the remainder is examined.

Theorem 5: If $f(x)$ has a continuous derivative of order $2n$ on $[a, b]$ then there exists a point ϕ in $[a, b]$ for which the remainder of the quadrature formula of the highest accuracy is

$$r(f) = \frac{f^{(2n)}(\phi)}{(2n)!} \int_a^b p(x) W^2(x) dx \quad (A.14)$$

These quadrature formulas of highest algebraic accuracy are used to evaluate two integrals which often occur in the specified problem of interest. It was because of these formulas that it was possible to write user-oriented computer programs using the Sommerfeld formulation that do not require unreasonable amounts of time.

a) Constant Weight Function:

The formulas of Gauss are historically the first formulas of the highest algebraic accuracy. These formulas are used to approximate the integral

$$\int_a^b f(x) dx \quad (A.15)$$

where $[a, b]$ is a finite segment and $p(x) \equiv 1$.

By a linear transformation we can transform an arbitrary segment $[a, b]$ into any standard segment we choose. In order to make use of the symmetry of the nodes x_k and coefficients A_k the segment would be made to be $[-1, +1]$. Thus it will be assumed that (A.15) can be transformed into the form

$$\int_{-1}^{+1} f_1(x) dx \quad (A.16)$$

The system of polynomials which are orthogonal on $[-1, +1]$ with respect to the constant weight function are the Legendre polynomials,

$$P_n(x) = \frac{1}{2^n n!} \frac{d^n (x^2 - 1)^n}{dx^n} \quad (A.17)$$

The quadrature formula of the highest accuracy

$$\int_{-1}^{+1} f(x) dx = \sum_{k=1}^n A_k^{(n)} f(x_k^{(n)}) \quad (A.18)$$

has for its n nodes the roots of the Legendre polynomial of degree n :

$$P_n(x_k^{(n)}) = 0 \quad (\text{A.19})$$

The coefficients A_k are then obtained as

$$A_k^{(n)} = \frac{2}{[1 - (x_k^{(n)})^2] [P_n'(x_k^{(n)})]^2} \quad (\text{A.20})$$

and since $W(x) = \frac{2^n (n!)^2}{(2n)!} P_n(x)$ to make the leading term of $W(x)$ unity, the remainder of the Gauss formula is obtained from (A.14) as

$$r(f) = \frac{2^{2n+1}}{(2n+1)(2n)!} \left[\frac{(n!)^2}{(2n)!} \right]^2 f^{(2n)}(\phi) \quad (\text{A.21})$$

where ϕ is a point in the segment $[-1, +1]$. Values of x_k and A_k for different n are given in the IBM-SSP [34].

b) Integrals of the Form $\int_0^\infty x^\alpha \exp(-x) f(x) dx$

The system of polynomials which are orthogonal on the semi-infinite axis $0 \leq x < \infty$ with respect to the function $x^\alpha \exp(-x)$ is the system of Chebyshev-Laguerre polynomials

$$L_n^{(\alpha)}(x) = (-1)^n x^{-\alpha} \exp(x) \frac{d^n}{dx^n} (x^{\alpha+n} \exp(-x)) \quad (\text{A.22})$$

A quadrature formula of the highest accuracy

$$\int_0^\infty x^\alpha \exp(-x) f(x) dx = \sum_{k=1}^n A_k f(x_k) + r(f) \quad (\text{A.23})$$

[34] IBM Scientific Subroutine Package (360A-CM-03X) Version II, Programmer's Manual, pp. 299-303.

must have as its nodes the roots of the Laguerre polynomial $L_n^{(\alpha)}(x)$, and the coefficient A_k can be found to be

$$A_k = \frac{(\alpha + n)!}{x_k [L_n^{(\alpha)}(x_k)]^2} \quad (\text{A.24})$$

Values of x_k and A_k for $\alpha = 0$ and for different n are given in the IBM-SSP [35]. The remainder of the quadrature formula $\alpha = 0$ is

$$r(f) = \frac{(n!)^2}{(2n)!} f^{(2n)}(\phi) \quad (\text{A.25})$$

where ϕ is a point between $[0, \infty]$.

[35] IBM-SSP, pp. 303-307.

Appendix B: ASYMPTOTIC EVALUATION OF INTEGRALS BY THE METHOD OF
STEEPEST DESCENT

The method of steepest descent (or the saddle point method) deals with the approximate evaluation of integrals of the form

$$I_{SD}(\rho) = \int_C F(\xi) \exp[-\rho f(\xi)] d\xi \quad (B.1)$$

for large values of ρ , where the contour C is such that the integrand goes to zero at the ends of the contour. The functions $f(\xi)$ and $F(\xi)$ are arbitrary analytic functions of the complex variable ξ .

The basic philosophy of the method of steepest descent is as follows: A path is selected in the complex ξ plane in such a way that the entire value of the integral is determined from a comparatively short portion of the path. Within certain limits, the contour of integration C may be altered to such a path without affecting the value of the integral. Then, the integrand is replaced by another, simpler function, which closely approximates the integrand over the essential portions of the path. The behavior of the new integrand outside the important portion of the path is of no concern. For real and positive values of ρ and for a general contour C the quantity $\rho f(\xi)$ is positive on some parts of the path and there are other regions where it is negative. The latter regions are more important since the integrand is larger, and in these regions, where the negative of the $\text{Re}[\rho f(\xi)]$ is largest, it is important to reduce oscillations. A contour is chosen along which the imaginary part of $[\rho f(\xi)]$ is constant in the region where the negative of its real part is largest. The path in the region where $\text{Re}[\rho f(\xi)]$ is greatest may be chosen so that $\text{Im}[\rho f(\xi)]$ varies if this turns out to be necessary to

complete the contour. In this way, the oscillations of the integral cause the least trouble.

This general philosophy can then be applied to evaluate the integral of (B.1). The type of integral encountered in this problem is of the form

$$I_{SD} = \int_{\Gamma_1} F(\beta) \exp[-jkR \cos(\beta-\theta)] d\beta \quad (B.2)$$

where Γ_1 is the path of integration as shown in Fig. 5. The saddle point occurs at $f'(\xi) = 0$, or at $\beta = \theta$ in this case. The path of integration is now determined from

$$\cos(\beta-\theta) = 1 - js^2/k$$

where s is real and $-\infty \leq s \leq +\infty$. The saddle point corresponds to $s = 0$. (B.2) can now be expressed in the following form

$$I_{SD} = \exp(-jkR) \int_{-\infty}^{\infty} \phi(s) \exp(-Rs^2) ds \quad (B.3)$$

where now $\phi(s) = F(\beta) \frac{d\beta}{ds}$. The details of evaluating (B.3) can be found in [36] and only the result is quoted.

$$I_{SD} = \left(\frac{2\pi}{kR}\right)^{1/2} \exp[j(\pi/4 - kR)] F(\theta) \left[1 + \frac{j}{2kR} \left\{\frac{1}{4} + \frac{F''(\theta)}{F(\theta)}\right\} + \dots\right] \quad (B.4)$$

Equation (B.4) is inapplicable if there is a pole near the saddle point θ . However, the method of steepest descent can be modified in such a way that

[36] L. B. Felsen and N. Marcuvitz, "Radiation and Scattering of Waves," Prentice Hall, New Jersey, 1973.

the presence of poles is taken into account from the very beginning.

Of special interest in the analysis will be an integral of the form

$$I(kR) = \int_{\Gamma_1} F_1(\beta) \exp[-jkR \cos(\beta-\theta)] d\beta \quad (B.5)$$

where Γ_1 is a path of integration in the complex β plane as shown in Fig. 5 and $F_1(\beta)$ now has a pole at β_p which is near θ . For large kR , the following method is applied: The pole is factored out from $F_1(\beta)$ by writing $F_1(\beta) = \frac{F(\beta)}{\sin(\frac{\beta-\beta_p}{2})}$. It is then argued by Clemmow [3], that

since $F(\beta)$ has no singularities in the vicinity of the saddle point it may be removed from under the integral sign with β equated to θ . Thus, the integral $I(kR)$ can be written as

$$I_{SD}(kR) = F(\theta) \int_{\Gamma_1} \frac{\exp[-jkR \cos(\beta-\theta)]}{\sin(\frac{\beta-\beta_p}{2})} d\beta \quad (B.6)$$

$$= F(\theta) \int_{\Gamma_0} \frac{\exp[-jkr \cos \alpha]}{\sin(\frac{\alpha+\theta-\beta_p}{2})} d\alpha \quad (B.7)$$

By reversing the sign of α as

$$I_{SD}(kR) = F(\theta) \int_{\Gamma_0} \frac{\exp[-jkR \cos \alpha]}{\sin(\frac{\theta-\alpha-\beta_p}{2})} d\alpha \quad (B.8)$$

and by adding (B.8) and (B.7) and then dividing by two, puts (B.6)

in the form

[37] P. C. Clemmow, "The Plane Wave Spectrum Representation of Electromagnetic Fields," Pergamon Press, New York 1966, pp. 46-58.

$$I_{SD}(kR) = 2 \sin \frac{\gamma}{2} F(\theta) \int_{\Gamma_0} \frac{\exp(-jkR \cos \alpha)}{\cos \alpha - \cos \gamma} \cos(\frac{\alpha}{2}) d\alpha$$

where $\gamma = \theta - \beta_P$. Changing the variable of integration from α to τ such that $\tau = \sqrt{2} \exp(-j\pi/4) \sin(\frac{\alpha}{2})$ the path Γ_1 is transformed to an integral from $-\infty$ to $+\infty$. Hence

$$I_{SD}(kR) = 2b \exp[j(3\pi/4 - kR)] F_1(\theta) \int_{-\infty}^{\infty} \frac{\exp(-kR\tau^2)}{\tau^2 + jb^2} d\tau \quad (B.9)$$

where $b = \sqrt{2} \sin \frac{\gamma}{2}$. Application of

$$\begin{aligned} \int_{-\infty}^{\infty} \frac{\exp(-x\tau^2)}{\tau^2 + jb^2} d\tau &= \\ &= \frac{\pi}{b} \exp[j(xb^2 - \pi/4)] \operatorname{erfc}(\sqrt{jxb^2}) \end{aligned}$$

from Gradshteyn and Ryzhik (p. 388, 3.466 No. 1) to (B.9), yields

$$I_{SD}(kR) = 2\pi \exp[j(\pi/2 - kR) - W^2] \operatorname{erfc}(jW) \quad (B.10)$$

where $W^2 = -jkRb^2 = -j2kR \sin^2(\frac{\theta - \beta_P}{2})$. Finally, application of (B.4) to the infinite integrals encountered in the Sommerfeld formulation yields the reflection coefficient method and that of (B.10) gives very good approximations for near fields.

REFERENCES

- [1] A. Banos, "Dipole Radiation in the Presence of a Conducting Half-Space," Pergamon Press, New York 1966.
- [2] E. K. Miller, A. J. Pozzio, G. J. Burke and E. S. Selden, "Analysis of Wire Antennas in the Presence of a Conducting Half-Space: Part I. The Vertical Antenna in Free Space," Canadian J. of Physics, vol. 50, pp. 879-888, 1972.
- [3] E. K. Miller, A. J. Pozzio, G. J. Burke and E. S. Selden, "Analysis of Wire Antennas in the Presence of Conducting Half-Space: Part II. The Horizontal Antenna in Free Space," Canadian J. of Physics, vol. 50, pp. 2614-2627, 1972.
- [4] D. L. Lager and R. J. Lytle, "Numerical Evaluation of Sommerfeld Integrals," Lawrence Livermore Laboratory, "Rept. UCRL-51688, October 23, 1974.
- [5] D. L. Lager and R. J. Lytle, "Fortran Subroutines for the Numerical Evaluation of Sommerfeld Integrals Unter Aderemem," Lawrence Livermore Laboratory, "Rept. UCRL-51821, May 21, 1975.
- [6] A. Sommerfeld, "Partial Differential Equations in Physics," Academic Press, New York, 1964.
- [7] R. E. Collin and F. J. Zucker, "Antenna Theory: Part 2, pp. 386-437, McGraw-Hill Book Co., New York 1969.
- [8] G. Tyas, "Radiation and Propagation of Electromagnetic Waves," Academic Press, New York, 1960.
- [9] L. M. Brekhovskikh, "Waves in Layered Media," Academic Press, New York.
- [10] T. K. Sarkar and J. E. Lewis, "Accurate Generation of Real Order and Argument Bessel and Modified Bessel Functions," Proc. IEE, p. 34, January 1973.
- [11] J. E. Lewis, T. K. Sarkar and P. D. O'Kelly, "Generation of Bessel Functions of Complex Order and Argument," Electron. Lett., vol. 7, No. 20. pp. 615-616.
- [12] Ref. [6], p. 189.
- [13] E. C. Jordan and K. G. Balmain, "Electromagnetic Waves and Radiating Systems," pp. 628-654, Prentice Hall, New Jersey, 1968.
- [14] R. F. Harrington, "Time Harmonic Electromagnetic Fields," McGraw-Hill, New York 1961, p. 133

- [15] H. H. Chao and B. J. Strait, "Computer Programs for Radiation and Scattering by Arbitrary Configurations of Bent Wires," Scientific Report No. 7 on Contract No. F19628-68-C-0180, AFCRL-70-0374; Syracuse University, Syracuse, New York, September 1970.
- [16] B. J. Strait, T. K. Sarkar and D. C. Kuo, "Programs for Analysis of Radiation by Linear Arrays of Vertical Wire Antennas Over Imperfect Ground," Technical Report TR-74-1 on Contract No. F19628-73-C-0047, AFCRL-TR-74-0042; Syracuse University, Syracuse, New York: January 1974.
- [17] T. K. Sarkar and B. J. Strait, "Analysis of Radiation by Wire Antennas Over Imperfect Ground," Scientific Report No. 6 on Contract F19628-73-C-0047, AFCRL-TR-75-0337; Syracuse University, Syracuse, New York: May 1975.
- [18] T. K. Sarkar, "Analysis of Radiation by Arrays of Vertical Wire Antennas Over Imperfect Ground (Reflection-Coefficient Method)," IEEE Trans. Ant. and Propagat. vol. AP-23, September 1975, p. 749.
- [19] T. K. Sarkar, "Analysis of Radiation by Arrays of Parallel Vertical Wire Antennas Over Plane Imperfect Ground (Sommerfeld Formulation)," IEEE Trans. Ant. and Propagat., (to be published).
- [20] J. R. Wait, "The Electromagnetic Fields of a Horizontal Dipole in the Presence of a Conducting Half-Space," Canadian J. of Phys., vol. 39, pp. 1017-1028, 1961.
- [21] T. K. Sarkar, "Analysis of Radiation by Arrays of Parallel Horizontal Wire Antennas Over Plane Imperfect Ground (Sommerfeld Formulation)," IEEE Trans. Ant. and Propagat., (to be published).
- [22] T. K. Sarkar and B. J. Strait, "Analysis of Radiation by Arrays of Parallel Horizontal Wire Antennas Over Imperfect Ground," Scientific Report No. 5 on Contract F19628-73-C-0047, AFCRL-TR-74-0538, Syracuse University, Syracuse, New York: September 1974.
- [23] T. K. Sarkar, "Analysis of Radiation by Arrays of Horizontal Wire Antennas Over Imperfect Ground," (Reflection Coefficient Method," IEEE Trans. Ant. and Propagat., (to be published).
- [24] T. K. Sarkar, "Analysis of Radiation by Arrays of Arbitrarily Oriented Wire Antennas Over Plane Imperfect Ground (Reflection Coefficient Method," IEEE Trans. Ant. and Propagat. (to be published).
- [25] B. J. Strait and D. C. Kuo, "Optimization Methods for Arrays of Parallel Wire Antennas," Scientific Report No. 18, Contract No. F19628-68-C-0180, AFCRL-72-0725, Syracuse University, Syracuse, New York: December 1972.

- [26] R. F. Harrington, "Field Computation by Moment Methods," The Macmillan Company, New York, 1968.
- [27] D. K. Cheng, "Optimization Techniques for Antenna Arrays," Proc. IEEE, No. 12, pp. 1664-1674, December 1971.
- [28] S. M. Sanzgiri and J. K. Butler, "Constrained Optimization of the Performance Indices of Arbitrary Array Antennas," IEEE Transactions on Antennas and Propagation, Vol. AP-19, No. 4, pp. 493-498, July 1971.
- [29] Y. T. Lo, S. W. Lee and D. H. Lee, "Optimization of Directivity and Signal to Noise Ratio of an Arbitrary Antenna Array," Proc. IEEE, Vol. 54, No. 8, pp. 1033-1045, August 1966.
- [30] L. P. Winkler and M. Schwartz, "A Fast Numerical Method for Determining the Optimum SNR of an Array Subject to a Q-Factor Constraint," IEEE Transaction of Antennas and Propagation, Vol. AP-20, No. 4, pp. 503-505, July 1972.
- [31] B. J. Strait, T. K. Sarkar and D. C. Kuo, "Special Programs for Analysis of Radiation by Wire Antennas," on Contract F19628-73-C-0047, AFCRL-73-0399, Syracuse University, Syracuse, NY 13210.
- [32] V. I. Krylov, "Approximate Calculations of Integrals," Macmillan Company, New York, 1962.
- [33] IBM Scientific Subroutine Package (360A-CM-03X) Version II, Programmer's Manual, pp. 299-303.
- [34] IBM - SSP, pp. 303-307.
- [35] L. B. Felsen and N. Marcuvitz, "Radiation and Scattering of Waves," Prentice Hall, New Jersey, 1973.
- [36] P. C. Clemmow, "The Plane Wave Spectrum Representation of Electromagnetic Fields," Pergamon Press, New York 1966, pp. 46-58.